Published in Chemical Geology 134, issues 1-3, 27-47, 1996
which should be used for any reference to this work

Metamorphic evolution of ultrahigh-pressure garnet peridotites from the Variscan Vosges Mts. (France)

Rainer Altherr *, Angelika Kalt

Mineralogisches Institut, Universität Heidelberg, Im Neuenheimer Feld 236, D-69120 Heidelberg, Germany

Abstract

In the Central Vosges Mts. (France) of the Variscan belt, Mg–Cr garnet peridotite bodies occur within the uppermost tectonometamorphic unit (Leptynitic granulites) as lenses in low-pressure/high-temperature metamorphic rocks. Neglecting late-stage serpentinization, the metamorphic evolution of these rocks was characterized by four stages. During stage I, the rocks were equilibrated at high pressures and temperatures (> 4.9 GPa/ > 950°C, in most cases > 1100°C), either within or near to the stability field of diamond. Stage II is documented by the formation of coronas around relict garnet with the assemblage orthopyroxene ± clinopyroxene ± amphibole + spinel ± plagioclase. During stage III, the remaining garnet was transformed to very fine-grained kelyphite consisting of orthopyroxene + amphibole + spinel ± plagioclase. Small relict garnet grains are preserved in one peridotite only. Stage IV corresponds to the late formation of tremolitic hornblende and chlorite which partially replaced the pseudomorphs after garnet or occur along cracks in the matrix of some rocks. Compositional zoning patterns of pyroxene porphyroclasts suggest that initial decompression was either accompanied by a moderate increase in temperature or nearly isothermal. Garnet breakdown textures and compositions of minerals grown during stages II and III also suggest rapid decompression at still elevated temperatures (1000–720°C).

Keywords: Garnet peridotite; Geothermobarometry; Vosges Mts.; Veriscan orogen; Ultrahigh-pressure metamorphism

1. Introduction

Garnet-bearing ultramafic rocks form volumetrically small albeit characteristic constituents of deeply eroded collision belts, like the Alps, the Caledonides, the Qinling–Dabie collision zone in eastern China, and the Variscan Belt of Central Europe (e.g., Evans and Trommsdorff, 1978; Medaris and Carswell, 1990; Zhang et al., 1994, 1995; Medaris et al., 1995a; Wang et al., 1995; see also Becker, 1996). Understanding the metamorphic evolution of these rocks is a key factor in elucidating the overall tectonothermal history of a collisional orogen.

So far, three hypotheses have been advocated to explain the origin of garnet-bearing ultramafic rocks. (1) Such rocks can be derived from high-temperature plagioclase or spinel peridotites that crystallized at fairly shallow levels and subsequently passed into the garnet peridotite or garnet pyroxenite stability field by cooling and/or subduction, thus indicating either a melting event within the upper mantle or crystal accumulation during the formation of a lay-

* Corresponding author.

ered intrusion within the lower continental crust (e.g., Carswell et al., 1983; Jamtveit, 1987a,b). (2) Garnet-bearing ultramafic rocks can also result from prograde high-pressure metamorphism of peridotites or serpentinites that had previously been emplaced into the crust as parts of ophiolitic complexes (e.g., Ernst, 1978; Evans and Trommsdorff, 1978; Obata, 1980). (3) Garnet-bearing ultramafic rocks may represent subcontinental lithospheric mantle material emplaced into the continental crust during collision and subsequent extensional collapse (e.g., Ernst, 1978; Carswell and Gibb, 1980; Medaris, 1980a,b).

It has been demonstrated that a collisional belt may host garnet-bearing ultramafic rocks of different origins. Examples are the Caledonides of western Norway (Medaris and Carswell, 1990, and references cited therein) and the Variscan belt (e.g., Medaris et al., 1990; O'Brien and Carswell, 1993; Kalt et al., 1995; Kalt and Altherr, 1996). As a consequence, knowledge on the origin and evolution of garnet-bearing ultramafic rocks may serve to distinguish tectonostratigraphic or tectonometamorphic units not recognized so far. In order to place constraints on the origin and evolution of garnet-bearing ultramafic rocks, field relations with the host rocks must be studied and P–T paths or even P–T–t paths must be established.

This paper describes the occurrence, mineral assemblages, and metamorphic evolution of six ultrahigh-pressure Mg–Cr garnet peridotites (without primary spinel) from the Central Vosges forming part of the Moldanubian zone of the Variscan collisional belt. An additional occurrence of garnet peridotite characterized by the presence of sapphirine as a breakdown product of garnet (Werling and Altherr, 1991) will be treated in a forthcoming paper.

2. Geological setting

The Vosges Mts. form part of the Variscan collisional belt which has been subdivided into a number of distinct zones, on account of regional differences in sedimentary, tectonic and metamorphic histories (Kossmat, 1927; Fig. 1). The metamorphic complexes of the Central Vosges belong to the Moldanubian zone. On the basis of fabrics, lithology, and metamorphic evolution, the medium- to high-grade metamorphic rocks of this area have been divided into four principal tectonostratigraphic units (Rey et al., 1989, 1991; Latouche et al., 1992): (1) the *Monotonous Group* at the base consisting of a sequence of 'anatectic paragneisses'; (2) the *Varied Group* comprising similar rocks with subordinate felsic orthogneisses, quartzites, amphibolites, and marbles; (3) a *migmatitic unit* thought to be derived from orthogneisses; and (4) *Leptynitic granulites* at the top consisting of relatively fine-grained, partly mylonitic felsic gneisses and relict granulites (Fig. 1). This subdivision is strikingly similar to the terrane concept established for the Bohemian Massif (see Medaris et al., 1995a,b for a review), units (3) and (4) of the Vosges corresponding to the migmatitic orthogneisses and the felsic to intermediate granulites of the composite Gföhl terrane in the Bohemian Massif, respectively.

The occurrences of high- (> 1.5 GPa) and ultrahigh-pressure (> 3.0 GPa) rocks in the Central Vosges seem to be restricted to the Monotonous Group (unit 1) and the Leptynitic granulites (unit 4). The only lens of amphibolitized eclogite described from the Vosges is enclosed in gneisses of the Monotonous Group (Hameurt, 1967) and may represent an equivalent of the numerous small bodies of medium-temperature eclogites within the Monotonous terrane of the Bohemian Massif (Medaris et al., 1995b; O'Brien and Vrána, 1995). Apart from the eclogite lens, the Monotonous Group contains spinel peridotites (Latouche et al., 1992). Garnet-bearing peridotites occur only within the Leptynitic granulites, where nine main localities have been recognized so far (Fig. 1). In terms of size, these peridotites range from lenses (or loose blocks) a few metres thick to large bodies of several hundred metres in areal extent. Two types of garnet-bearing peridotites have been identified (Altherr and Kalt, 1995): garnet peridotite with no evidence for pre-existing spinel (seven occurrences) and garnet-spinel peridotites with spinel occurring in garnet and in the matrix (two occurrences).

Like elsewhere in the Moldanubian zone, the high- and ultrahigh-pressure rocks in the Central Vosges and their country rocks have been subject to an intensive low-pressure/high-temperature overprint. This event produced sillimanite-cordierite gneisses associated with intrusive granitoids and

variably developed ductile shear zones (Rey et al., 1991; Latouche et al., 1992). Thus, the principal fabric in the Central Vosges gneiss complexes postdates high- and ultrahigh-pressure metamorphism; it developed after substantial exhumation of the high- and ultrahigh-pressure rocks. Although rare kyanite

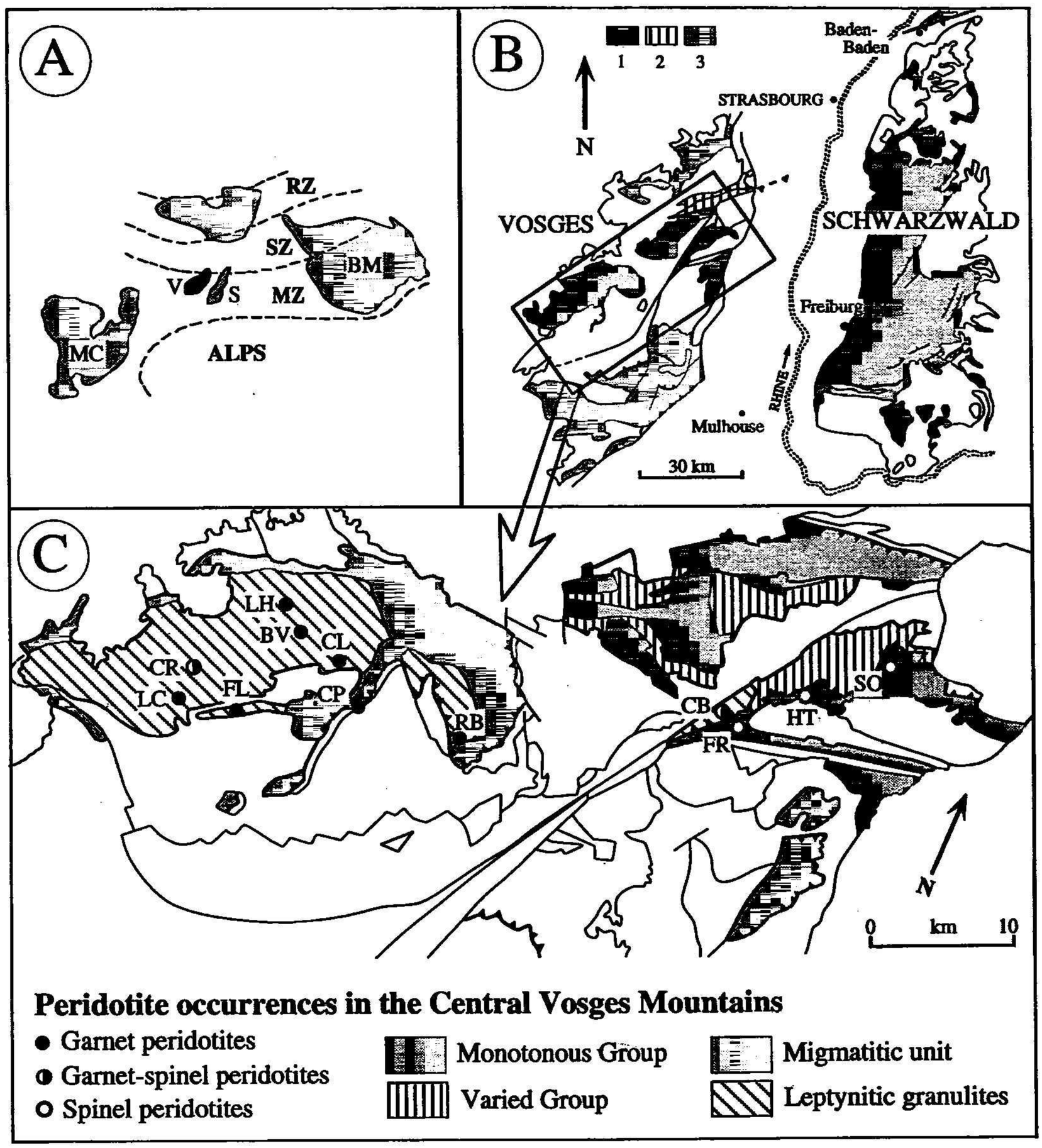

Fig. 1. (A) Location of the Vosges Massif within the frame of Variscan Europe: *BM* = Bohemian Massif; *MC* = Massif Central; *MZ* = Moldanubian zone; *RZ* = Rhenohercynian zone; *S* = Schwarzwald; *SZ* = Saxothuringian zone; *V* = Vosges Mountains. (B) Vosges Mountains and Schwarzwald: *1* = gneiss complexes; *2* = low-grade Cambro–Silurian metaclastics; *3* = lower Carboniferous sedimentary and volcanic rocks (partly metamorphosed). (C) Tectonometamorphic units and peridotite localities in the Central Vosges: *BV* = Belle Vue; *CB* = Col des Bagenelles; *CL* = Champ de Laxet; *CP* = Col de Perthuis; *CR* = Crébimont; *FL* = Flaconnières; *FR* = Faurupt; *HT* = Hohltann; *LC* = La Charme; *LH* = Laveline-du-Houx; *RB* = Roche des Bruyères; *SO* = Sobache. Carboniferous granites, low-grade metamorphic rocks, and Permian to Mesozoic rocks are undifferentiated; geological boundaries of these units are given for better orientation.

relicts in gneisses of the Monotonous and Varied Groups and relictic granulites in the unit of 'Leptynitic granulites' (Hameurt, 1967; Fluck, 1980; Fabriès and Latouche, 1988) indicate higher pressures prior to the later overall low-pressure equilibration, no evidence of a former high- or even ultra-high-pressure stage has been found so far in the gneissic country rocks.

Apart from geologically meaningless Rb–Sr whole rock data (Bonhomme, 1965, 1967; Hameurt and Vidal, 1973; Bonhomme and Fluck, 1981) and scarce K–Ar and Ar–Ar mineral dates (Faul and Jäger, 1963; Montigny et al., 1983; Montigny and Thuizat, 1989) there are no isotopic age data available to constrain the geological evolution in the Central Vosges. By analogy with the Gföhl unit in the Bohemian Massif (see Medaris et al., 1995a, for a review) and the neighbouring Schwarzwald (Kalt et al., 1994a,b and unpubl. results), it seems likely that both high- to ultrahigh-pressure metamorphism and regional low-pressure/high-temperature metamorphism in the Vosges took place during the Early Carboniferous. The peak of high-temperature metamorphism (at ~ 334 Ma B.P., Kalt et al. unpubl. results) was immediately followed by the intrusion of granitoid plutons as suggested by K–Ar and Ar–Ar cooling ages (Montigny and Thuizat, 1989).

3. Analytical techniques

A Camebax SX51 microprobe equipped with 5 wavelength-dispersive spectrometers and an energy-dispersive system was used for mineral analyses. Operating parameters were 20 nA beam current, 15 kV accelerating voltage, 10 s counting time for all elements except Ti, Cr, Si in olivine (20 s), Ni, Ca, Al in olivine (30 s), Mg, Ca, Al in spinel (20 s), and Ti in spinel (30 s). Between 290 and 485 individual point analyses were carried out for each sample, and in addition traverses (up to 540 point analyses) and chemical mapping were performed. Kelyphites were analysed by using a defocused electron beam (diameter 50 μm). Kelyphite compositions (Tables 3 and 6)

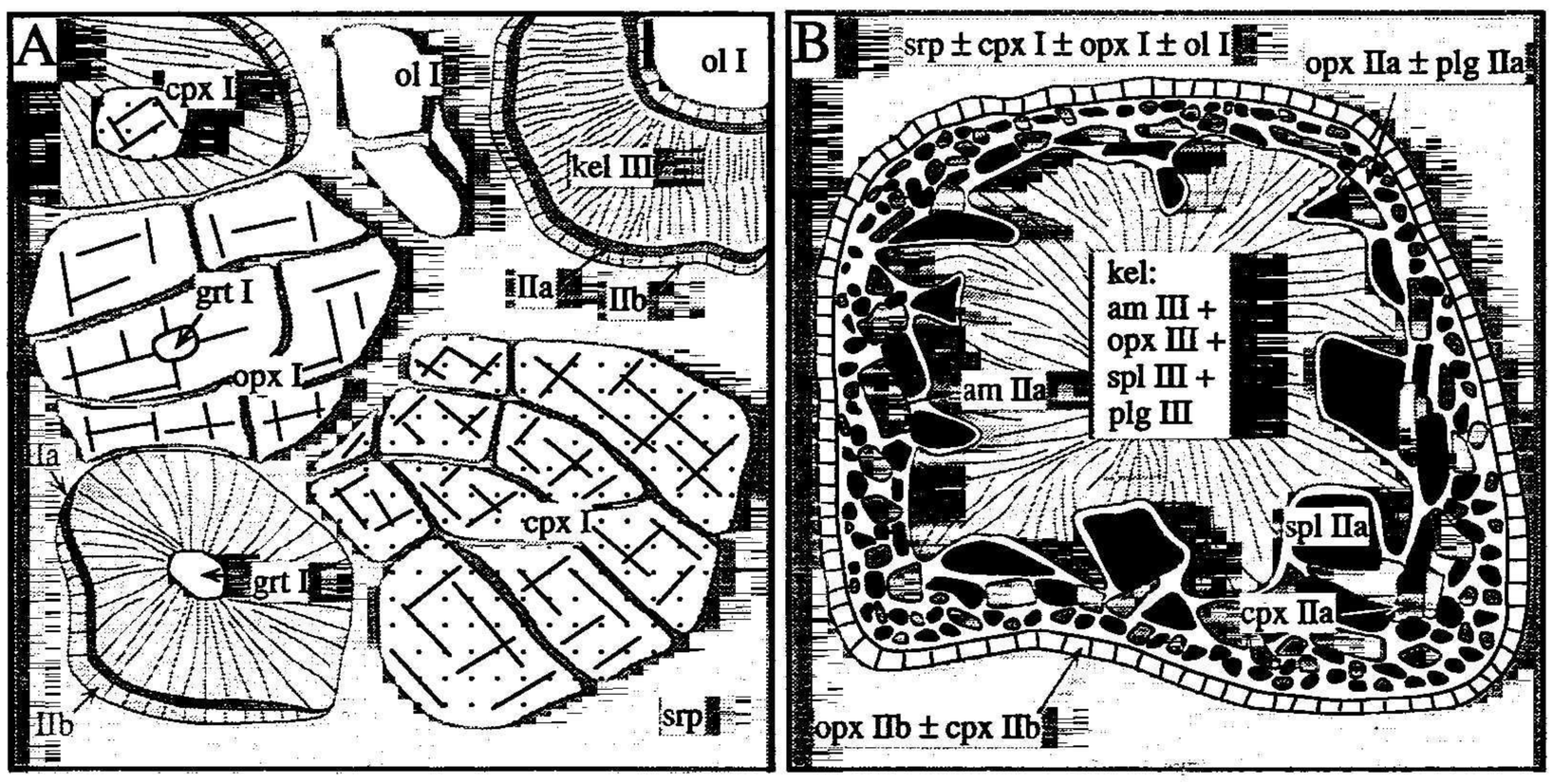

Fig. 2. Schematic representation of some important textural features. For mineral abbreviations and detailed description see section on textures and mineral compositions in the text. (A) Peridotite Belle Vue (BV) with pseudomorphs after garnet and cpx I, opx I, and ol I. Kelyphite (kel III) consists of vermicular opx III, cpx III, am III, and spl III and contains inclusions of relict cpx I, opx I, ol I, and grt I. Adjacent to olivine or serpentine (srp) a seam of granoblastic opx IIb ± cpx IIb has formed. In some pseudomorphs, a very thin and fine-grained layer of opx IIa, cpx IIa, am IIa, and spl IIa is present between the external granoblastic layer IIb and the internal kelyphite. Edge of drawing represents ~ 3 mm. (B) Pseudomorph after garnet in peridotites CL, CP, FL, and LC. A fine-grained kelyphite (opx III ± cpx III ± am III + spl III + plg III) is mantled by a corona consisting of two layers: an internal layer formed by granoblastic aggregates of opx IIa + am IIa ± cpx IIa + spl IIa ± plg IIa and a thin external layer of opx IIb ± cpx IIb. Note the sharp interface between kelyphite and the two-layer corona. Matrix consists of srp and relict cpx I, opx I, and ol I. Edge of drawing represents ~ 1 cm.

Table 1
Chemical variations in minerals from garnet peridotites

Mineral	Parameter	BV	CL	CP	FL	LC	RB
Opx I, cores	Al_2O_3	0.18–0.33	0.68–0.98	0.71–0.99	0.82–1.07	0.61–0.75	1.00–1.31
	Cr_2O_3	0.01–0.20	0.03–0.21	0.06–0.21	0.08–0.33	0.04–0.20	0.14–0.28
	CaO	0.19–0.36	0.47–0.59	0.49–0.61	0.54–0.72	0.46–0.69	0.53–0.82
	X_{Mg}	0.900–0.918	0.885–0.898	0.895–0.903	0.896–0.901	0.899–0.908	0.900–0.907
Opx I, rims	Al_2O_3	0.32–1.18	1.04–1.82	1.02–1.58	1.05–1.22	0.70–1.62	1.13–1.51
	Cr_2O_3	0.04–0.37	0.12–0.25	0.12–0.25	0.16–0.28	0.08–0.25	0.19–0.29
	CaO	0.29–0.47	0.28–0.65	0.26–0.62	0.39–0.59	0.33–0.52	0.36–0.59
	X_{Mg}	0.895–0.914	0.889–0.901	0.893–0.905	0.896–0.902	0.893–0.904	0.898–0.906
Opx IIa	Al_2O_3	1.92	4.62–6.94	4.97–9.21	2.50–8.05	3.18–7.62	6.19–8.90
	Cr_2O_3	0.31	0.36–0.57	0.25–0.75	0.24–0.64	0.27–0.54	0.40–0.63
	CaO	0.34	0.18–0.37	0.26–0.85	0.29–0.90	0.19–0.61	0.31–0.61
	X_{Mg}	0.910	0.869–0.890	0.869–0.888	0.852–0.883	0.869–0.890	0.863–0.872
Opx IIb	Al_2O_3	1.78–3.98	2.25–5.85	1.62–5.69	3.02–5.85	3.38–4.42	1.41–3.63
	Cr_2O_3	0.01–0.35	0.30–0.45	0.02–0.35	0.18–0.48	0.19–0.32	0.10–0.26
	CaO	0.31–0.44	0.23–0.71	0.28–0.60	0.48–0.83	0.40–0.55	0.44–0.70
	X_{Mg}	0.891–0.903	0.873–0.898	0.887–0.902	0.871–0.890	0.882–0.889	0.892–0.905
Opx III	Al_2O_3	5.37–6.88	n.a.	2.76–3.70	n.a.	2.33–4.92	–
	Cr_2O_3	0.72–0.82	n.a.	0.23–0.27	n.a.	0.11–0.31	–
	CaO	0.30–0.34	n.a.	0.25–0.29	n.a.	0.23–0.35	–
	X_{Mg}	0.895–0.903	n.a.	0.888–0.891	n.a.	0.881–0.885	–
Cpx I, cores	Al_2O_3	1.07–1.67	2.68–3.21	2.56–3.32	2.74–3.48	2.66–3.14	2.66–3.26
	Cr_2O_3	0.85–1.18	0.64–0.90	0.73–0.99	0.67–1.14	0.68–0.95	0.88–0.97
	CaO	20.3–22.0	18.1–19.2	18.7–20.9	18.3–19.5	18.5–19.6	18.4–19.7
	Na_2O	1.10–1.82	1.51–2.32	1.20–1.93	1.00–1.98	1.66–2.26	1.51–1.80
	X_{Mg}	0.896–0.923	0.891–0.908	0.904–0.925	0.894–0.916	0.893–0.910	0.895–0.917
Cpx I, rims	Al_2O_3	1.10–2.84	2.70–4.06	2.80–3.96	2.82–3.43	2.66–3.12	2.63–3.41
	Cr_2O_3	0.66–1.20	0.46–0.97	0.76–0.97	0.66–1.08	0.67–0.94	0.40–1.29
	CaO	19.6–21.8	18.6–23.1	19.7–23.2	19.3–22.3	18.5–21.5	19.0–22.9
	Na_2O	0.61–1.82	0.59–2.07	1.04–1.97	0.87–1.71	0.76–2.03	0.82–1.70
	X_{Mg}	0.896–0.929	0.890–0.934	0.905–0.927	0.905–0.922	0.902–0.926	0.918–0.942
Cpx IIa	Al_2O_3	1.70–7.53	–	–	–	3.47–3.74	9.16–10.49
	Cr_2O_3	1.18–1.67	–	–	–	0.95–0.97	0.73–0.84
	CaO	23.6–24.4	–	–	–	19.9–20.1	20.9–21.2
	Na_2O	0.27–0.76	–	–	–	0.62–0.73	1.22–1.42
	X_{Mg}	0.916–0.936	–	–	–	0.908–0.912	0.915–0.922
Cpx IIb	Al_2O_3	2.46–2.96	–	–	4.01–6.95	–	–
	Cr_2O_3	0.86–1.32	–	–	0.69–0.74	–	–
	CaO	21.8–23.1	–	–	22.3–23.4	–	–
	Na_2O	0.72–1.11	–	–	0.61–0.82	–	–
	X_{Mg}	0.908–0.923	–	–	0.897–0.921	–	–
Cpx III	Al_2O_3	5.14–7.70	–	–	–	–	–
	Cr_2O_3	0.46–1.36	–	–	–	–	–
	CaO	23.2–23.4	–	–	–	–	–
	Na_2O	0.32–0.65	–	–	–	–	–
	X_{Mg}	0.896–0.920	–	–	–	–	–
Ol I	X_{Mg}	0.894–0.906	0.876–0.904	0.887–0.899	0.892–0.897	0.890–0.903	0.890–0.899

Table 1 (continued)

Mineral	Parameter	BV	CL	CP	FL	LC	RB
Grt I	Cr_2O_3	1.77–3.35	–	–	–	–	–
	CaO	4.20–4.68	–	–	–	–	–
	X_{Mg}	0.728–0.780	–	–	–	–	–
Spl IIa	X_{Cr}	0.218–0.257	0.065–0.105	0.061–0.068	0.073–0.087	0.059–0.087	0.069–0.076
	X_{Mg}	0.632–0.662	0.749–0.765	0.742–0.751	0.680–0.729	0.717–0.747	0.656–0.969
Spl III	X_{Cr}	0.032–0.134	n.a.	0.076–0.079	n.a.	n.a.	–
	X_{Mg}	0.728–0.777	n.a.	0.754–0.763	n.a.	n.a.	–
Am IIa	TiO_2	0.51–0.65	2.18–3.52	0.61–1.94	4.20–4.98	4.30–5.03	1.31–2.22
	Al_2O_3	12.2–12.8	13.8–14.9	15.3–16.5	13.4–14.2	13.0–14.2	15.3–16.6
	X_{Mg}	0.900–0.911	0.887–0.902	0.862–0.900	0.843–0.857	0.862–0.878	0.885–0.923
	Na_2O	2.47–2.53	2.91–3.38	3.62–3.99	3.34–3.58	2.70–2.92	1.89–2.38
Am III	TiO_2	0.53–1.42	3.05	4.89–5.23	n.a.	4.57–4.86	–
	Al_2O_3	14.0–15.8	14.4	13.4–15.5	n.a.	13.4–13.5	–
	X_{Mg}	0.892–0.910	0.890	0.867–0.888	n.a.	0.868–0.874	–
	Na_2O	2.89–3.64	3.33	3.26–3.36	n.a.	2.70–2.79	–
Am IV	TiO_2	–	–	0.17–0.45	–	–	0.19–0.37
	Al_2O_3	–	–	2.60–5.72	–	–	2.22–2.35
	X_{Mg}	–	–	0.905–0.926	–	–	0.953–0.960
	Na_2O	–	–	0.83–1.62	–	–	0.40–0.70
Chl IVa	Al_2O_3	2.12–8.99	–	7.89–9.00	–	–	–
	X_{Mg}	0.865–0.907	–	0.853–0.876	–	–	–
Chl IVb	Al_2O_3	–	–	17.4–20.2	14.3	–	18.7
	X_{Mg}	–	–	0.927–0.933	0.919	–	0.935

n.a. = not analyzed; – = not present.

represent mean values of about 10–15 analyses taken at various positions within kelyphites. PAP correction was applied to all data. Natural and synthetic silicate and oxide standards were used for calibration.

4. Textures and mineral compositions

Although all peridotites have been extensively retrogressed, primary textures and mineral assemblages have been partially preserved and the metamorphic evolution of these rocks can be discerned.

The peridotite from *Belle Vue* (*BV*) is medium- to fine-grained and only weakly foliated. Millimetre-sized grains of orthopyroxene (opx I), clinopyroxene (cpx I), relict olivine (ol I), and pseudomorphed garnet frequently intergrown with each other are embedded in serpentine. Some opx I grains contain small inclusions of relict garnet (grt I). Smaller isolated pyroxene grains may represent neoblasts as suggested by their compositions (see below). Pseudomorphs after garnet (Fig. 2A) are kelyphites composed of orthopyroxene (opx III), amphibole (am III), spinel (spl III), and minor clinopyroxene (cpx III), whereby opx III is often replaced by chlorite (chl IVa). Relict grt I, opx I, and cpx I may be preserved in the inner parts of kelyphites, the grain size of these kelyphites increasing rimwards. Along their contacts with serpentine or relict ol I, kelyphites are rimmed by coronas consisting of two layers: an internal very thin and fine-grained layer of granular amphibole (am IIa), clinopyroxene (cpx IIa), orthopyroxene (opx IIa), and spinel (spl IIa), and an external layer of granular orthopyroxene (opx IIb) and minor clinopyroxene (cpx IIb).

Orthopyroxene I grains have uniform X_{Mg} (= Mg/(Mg + Fe)) but show zoning in Al, Cr, and Ca with all elements increasing from core to rim (Tables 1 and 2, Fig. 3). Due to the very fine grain size of opx IIa only one grain could be analyzed. It has slightly higher abundances of Al_2O_3 than the rims of opx I grains. Opx IIb is characterized by variable Al_2O_3 and CaO contents. Opx III is high in Al_2O_3 and low in CaO (Tables 1 and 2).

Clinopyroxene I grains are also zoned, with core compositions being fairly uniform (Tables 1 and 2, Fig. 3). Rim compositions are more variable and are characterized by higher Al_2O_3 but lower CaO and Na_2O contents. There is no systematic difference in X_{Mg} between cpx I cores and rims. Cpx IIa and cpx III grains show variable compositions with high contents of Al_2O_3 and CaO but low contents of Na_2O.

Relict ol I grains are unzoned and show uniform X_{Mg} (Tables 1 and 2). Relict grt I is relatively low in CaO and shows variable Cr_2O_3 contents and X_{Mg}.

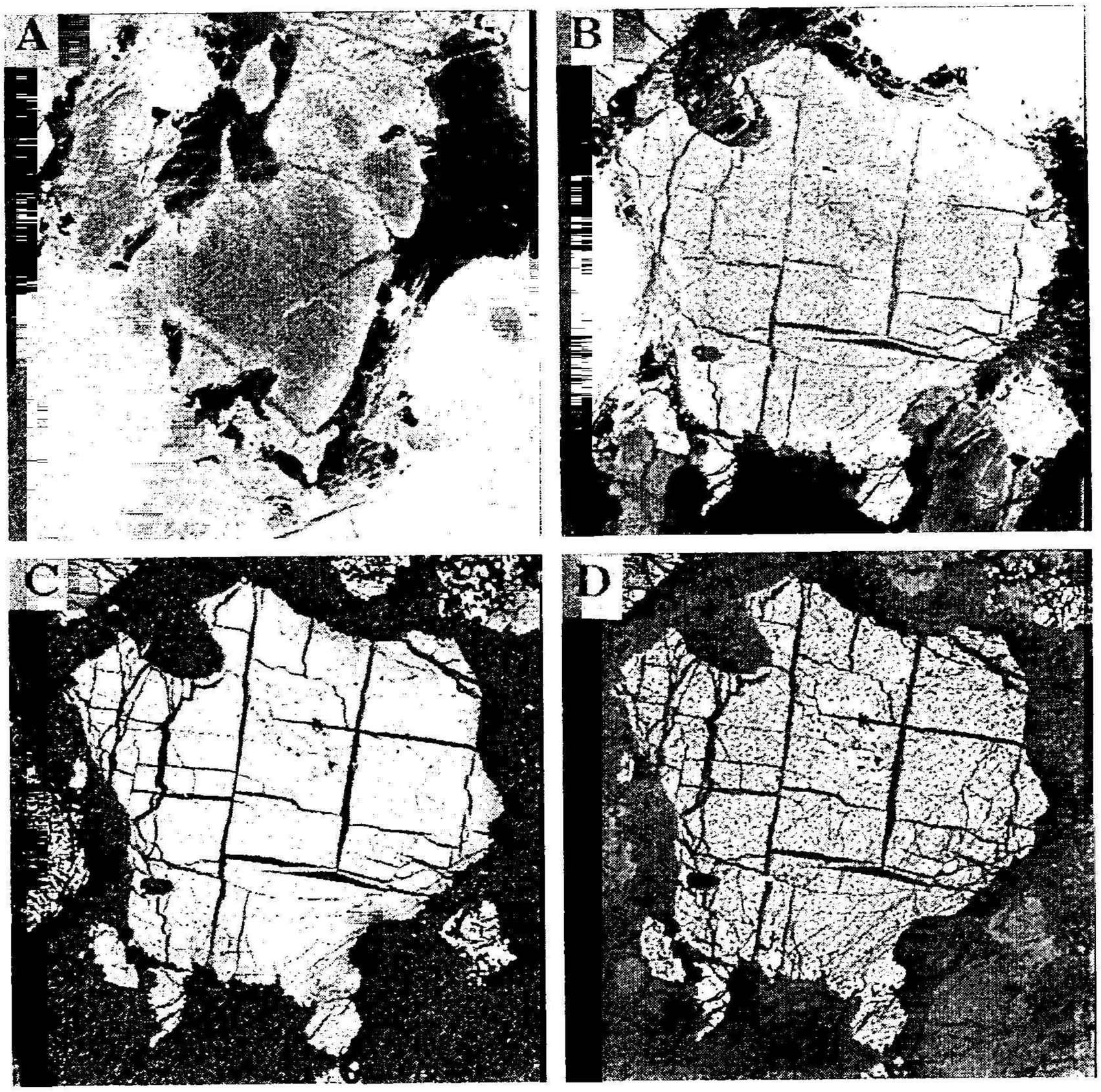

Fig. 3. X-ray map for Al in opx I (A) and Al (B), Na (C) and Ca (D) in cpx I in garnet peridotite BV. Light colours indicate high, dark colours low element abundances. See section on textures and mineral compositions in the text and Table 1 for further explanation. Edges of photos represent 1.8 mm.

Table 2
Representative electron microprobe analyses of minerals from garnet peridotite BV

	opx Ic	opx Ir	cpx Ic	cpx Ir	grt I	ol I	opx IIa	cpx IIa	am IIa	spl IIa	opx IIb	am III	opx III	cpx III	spl III
SiO_2	58.38	57.33	55.34	55.23	41.74	40.64	57.74	51.22	45.37	0.02	55.57	42.56	52.53	51.02	0.06
TiO_2	0.00	0.09	0.05	0.03	0.14	0.00	0.02	0.33	0.65	0.04	0.07	1.42	0.03	0.37	0.01
Al_2O_3	0.23	0.85	1.22	1.40	20.52	0.01	1.92	5.08	12.50	47.05	3.98	14.65	6.88	5.14	55.07
Cr_2O_3	0.10	0.18	1.08	0.86	3.10	0.02	0.31	0.76	1.36	19.62	0.35	0.38	0.72	1.36	12.72
Fe_2O_3	n.c.	n.c.	n.c.	n.c.	n.c.	n.c.	n.c.	n.c.	0.93	1.43	n.c.	0.53	n.c.	n.c.	0.10
FeO	5.68	6.31	2.56	2.83	10.32	9.72	6.13	2.58	2.88	14.12	6.65	3.42	6.70	2.45	11.83
MnO	0.13	0.13	0.06	0.05	0.79	0.14	0.15	0.13	0.05	0.08	0.13	0.07	0.18	0.04	0.07
NiO	n.a.	n.a.	n.a.	n.a.	n.a.	0.37	n.a.	n.a.	n.a.	n.a.	n.a.	n.a.	n.a.	n.a.	n.a.
MgO	35.28	34.46	16.75	18.82	19.34	48.84	34.56	15.88	18.74	16.25	33.02	18.14	32.09	15.92	18.57
CaO	0.33	0.40	21.91	20.80	4.60	0.01	0.34	23.38	12.46	0.01	0.44	12.56	0.32	23.26	0.02
Na_2O	0.00	0.03	1.31	0.61	0.00	0.00	0.02	0.25	2.53	0.00	0.02	3.49	0.03	0.32	0.00
K_2O	0.01	0.01	0.02	0.01	0.00	0.00	0.00	0.00	0.03	0.00	0.00	0.03	0.01	0.00	0.00
H_2O	–	–	–	–	–	–	–	–	2.12	–	–	2.10	–	–	–
Total	100.14	99.79	100.30	100.64	100.55	99.75	101.19	99.61	99.62	98.62	100.23	99.35	99.49	99.88	98.45
Si	2.000	1.980	1.999	1.998	3.004	0.999	1.964	1.873	6.414	.001	1.915	6.078	1.831	1.863	0.001
Ti	0.000	0.002	0.001	0.001	0.007	0.000	0.000	0.009	0.069	0.001	0.002	0.153	0.001	0.010	0.000
Al	0.009	0.035	0.052	0.059	1.741	0.000	0.077	0.219	2.082	1.538	0.162	2.466	0.283	0.221	1.727
Cr	0.003	0.005	0.031	0.024	0.176	0.000	0.008	0.022	0.152	0.430	0.010	0.042	0.020	0.039	0.268
Fe^{3+}	n.c.	n.c.	n.c.	n.c.	n.c.	n.c.	n.c.	n.c.	0.099	0.030	n.c.	0.057	n.c.	n.c.	0.002
Fe^{2+}	0.163	0.182	0.077	0.085	0.621	0.200	0.174	0.079	0.340	0.327	0.192	0.409	0.195	0.075	0.263
Mn	0.004	0.004	0.002	0.005	0.048	0.003	0.004	0.004	0.006	0.002	0.004	0.009	0.005	0.001	0.002
Ni	n.a.	n.a.	n.a.	n.a.	n.a.	0.007	n.a.	n.a.	n.a.	n.a.	n.a.	n.a.	n.a.	n.a.	n.a.
Mg	1.802	1.774	0.902	1.006	2.076	1.790	1.752	0.866	3.949	0.672	1.696	3.863	1.668	0.866	0.736
Ca	0.012	0.015	0.848	0.799	0.354	0.000	0.012	0.916	1.887	0.000	0.016	1.922	0.012	0.910	0.000
Na	0.000	0.002	0.092	0.042	0.000	0.000	0.001	0.017	0.695	0.000	0.001	0.966	0.002	0.023	0.000
K	0.000	0.001	0.001	0.000	0.000	0.000	0.000	0.000	0.006	0.000	0.000	0.005	0.000	0.000	0.000
Total	3.993	4.000	4.005	4.001	8.027	2.999	3.992	4.005	15.699	3.001	3.998	15.970	4.017	4.008	2.999
XMg	0.917	0.907	0.921	0.922	0.770	0.899	0.910	0.916	0.921	0.673	0.898	0.904	0.895	0.920	0.727

Formula calculations on the basis of 6 oxygens for cpx and opx, 4 oxygens for ol, 12 oxygens for grt, 4 oxygens and 3 cations for spl, and 15 cations without Na + K for am. X_{Mg} for grt, ol, opx, and cpx calculated on the assumption that all Fe is divalent; X_{Mg} for spl and am is calculated using $Fe^{2+}/(Fe^{2+}+Fe^{3+})$ ratio as given by formula calculation. H_2O for am was calculated assuming 2 OH per formula unit. For mineral abbreviations see section on textures and mineral compositions; c = core, r = rim, n.a. = not analyzed, n.c. = not calculated.

Spinel IIa has higher X_{Cr} (= Cr/(Cr + Al)) and lower X_{Mg} than spl III (Tables 1 and 2). Amphibole IIa is a pargasitic hornblende, while am III is a pargasite. Chlorite IVa replacing opx III shows variable Al_2O_3.

The peridotites from *Champ de Laxet* (*CL*), *Col de Perthuis* (*CP*), *Flaconnières* (*FL*), *La Charme* (*LC*), *and Roche des Bruyères* (*RB*) display similar textures and mineral assemblages. They are all characterized by a porphyroclastic texture in which large pseudomorphed garnets (up to 1 cm), smaller strained pyroxene porphyroclasts (opx I, cpx I), and a few pyroxene neoblasts are set in a fine-grained matrix of orthopyroxene, clinopyroxene, olivine, and late-stage serpentine. In one sample (peridotite RB), cpx I porphyroclasts are fringed by late-stage tremolitic hornblende (am IV). Garnet pseudomorphs are round and undeformed (Fig. 2B). Most of their volume is taken up by an extremely fine-grained kelyphite composed of amphibole (am III), orthopyroxene (opx III), spinel (spl III), and plagioclase (plg III). Kelyphites are surrounded by coronas consisting of two

Table 3
Representative electron microprobe analyses of minerals from garnet peridotite CL

	opx Ic	opx Ir	cpx Ic	cpx Ir	kel	grt Z	grt mc	ol I	opx IIa	am IIa	spl IIa	opx IIb	am III
SiO_2	57.14	55.95	55.34	52.57	44.30	42.03	41.53	40.33	53.45	42.02	0.04	54.83	42.47
TiO_2	0.07	0.07	0.27	0.26	0.20	0.15	0.12	0.03	0.15	2.64	0.02	0.12	3.05
Al_2O_3	0.69	1.25	2.74	3.23	21.44	21.95	21.92	0.00	5.77	14.94	60.78	3.48	14.44
Cr_2O_3	0.14	0.15	0.84	0.79	1.53	2.72	1.59	0.02	0.40	1.04	6.88	0.28	0.94
Fe_2O_3	n.c.	n.c.	n.c.	n.c.	n.c.	n.c.	0.00	n.c.	n.c.	n.c.	0.14	n.c.	0.00
FeO	7.22	7.05	2.97	2.32	6.29	11.31	11.66	11.74	7.63	3.72	11.07	7.42	3.69
MnO	0.22	0.20	0.11	0.10	0.14	0.69	0.30	0.20	0.16	0.08	0.13	0.27	0.10
NiO	n.a.	n.a.	n.a.	n.a.	n.a.	n.a.	0.00	0.39	n.a.	n.a.	n.a.	n.a.	n.a.
MgO	33.32	34.22	16.75	16.33	19.68	18.57	17.73	47.12	32.32	17.04	19.64	33.36	16.74
CaO	0.53	0.52	19.38	23.13	4.77	3.93	5.15	0.03	0.23	12.18	0.03	0.24	11.72
Na_2O	0.01	0.01	2.12	0.85	1.15	n.d.	0.00	0.00	0.02	3.12	0.00	0.03	3.33
K_2O	0.00	0.00	0.01	0.00	0.01	n.d.	0.00	0.00	0.00	0.38	0.00	0.01	0.06
H_2O	–	–	–	–	–	–	–	–	–	2.09	–	–	2.09
Total	99.34	99.42	100.53	99.58	99.51	101.35	100.00	99.86	100.13	99.25	98.73	100.04	98.63
Si	1.990	1.951	1.985	1.921	3.135	2.998	3.005	1.000	1.856	6.020	0.001	1.904	6.101
Ti	0.002	0.002	0.007	0.007	0.010	0.008	0.007	0.001	0.004	0.284	0.000	0.003	0.329
Al	0.028	0.051	0.116	0.139	1.788	1.845	1.869	0.000	0.236	2.523	1.854	0.143	2.445
Cr	0.004	0.004	0.024	0.023	0.086	0.153	0.091	0.000	0.011	0.118	0.141	0.008	0.106
Fe^{3+}	n.c.	n.c.	n.c.	n.c.	n.c.	n.c.	0.000	n.c.	n.c.	0.000	0.003	n.c.	0.000
Fe^{2+}	0.210	0.206	0.089	0.071	0.372	0.675	0.705	0.243	0.221	0.446	0.240	0.216	0.443
Mn	0.007	0.006	0.003	0.003	0.008	0.042	0.018	0.004	0.005	0.010	0.003	0.008	0.012
Ni	n.a.	n.a.	n.a.	n.a.	n.a.	n.a.	0.000	0.008	n.a.	n.a.	n.a.	n.a.	n.a.
Mg	1.730	1.779	0.896	0.890	2.076	1.974	1.913	1.742	1.674	3.638	0.758	1.727	3.584
Ca	0.020	0.019	0.745	0.906	0.362	0.300	0.399	0.001	0.008	1.869	0.001	0.009	1.804
Na	0.001	0.001	0.148	0.060	0.158	n.a.	0.000	0.000	0.001	0.867	0.000	0.002	0.927
K	0.000	0.000	0.000	0.000	0.001	n.a.	0.000	0.000	0.000	0.069	0.000	0.000	0.010
Total	3.992	4.019	4.013	4.020	7.996	7.995	8.007	2.999	4.016	15.844	3.001	4.020	15.761
X_{Mg}	0.892	0.896	0.910	0.926	0.848	0.745	0.731	0.878	0.883	0.891	0.760	0.889	0.890

Formula calculations on the basis of 6 oxygens for cpx and opx, 4 oxygens for ol, 12 oxygens for grt, 4 oxygens and 3 cations for spl, and 15 cations without Na + K for am. X_{Mg} for grt, ol, opx, and cpx calculated on the assumption that all Fe is divalent; X_{Mg} for spl and am is calculated using $Fe^{2+}/(Fe^{2+} + Fe^{3+})$ ratio as given by formula calculation. H_2O for am was calculated assuming 2 OH per formula unit. For mineral abbreviations see section on textures and mineral compositions; c = core, r = rim, n.a. = not analyzed, n.c. = not calculated. Analyses grt Z is a garnet composition from an ultrahigh-pressure peridotite from eastern China (table 4 in Zhang et al., 1994); grt mc is a model garnet composition derived from an average kelyphite composition in garnet peridotite CL.

layers. The internal layers are formed by granoblastic aggregates of orthopyroxene (opx IIa), amphibole (am IIa), Cr–Al spinel (spl IIa), and sometimes clinopyroxene (cpx IIa) and/or plagioclase (plg IIa). If present, the latter usually occurs along grain boundaries between spl IIa and opx IIa. Opx IIa may be partially replaced by chlorite (chl IVa). The interface between the kelyphite and this granoblastic layer is always sharp and has irregular lobate outlines. Moving outwards from the kelyphite, grain sizes decrease. The thin external layer is formed by granoblastic orthopyroxene (opx IIb), in some cases (e.g. FL) accompanied by clinopyroxene (cpx IIb). Kelyphites may contain inclusions of opx I and cpx I grains. In peridotites CP and RB, pseudomorphs after garnet may be partially or completely transformed to aggregates of decussate chlorite (chl IVb), amphibole (am IV), and minor graphite and carbonate. This assemblage is also found along cracks in the matrix and predates serpentinization.

Larger opx I porphyroclasts show fairly uniform compositions with only minor zoning at their rims. Homogeneous cores are characterized by low Al_2O_3 and Cr_2O_3 contents, comparatively high CaO con-

Table 4
Representative electron microprobe analyses of minerals from garnet peridotite CP

	opx Ic	opx Ir	cpx Ic	cpx Ir	ol I	opx IIa	am IIa	spl IIa	opx IIb	opx III	am III	spl III	am IV	chl IVa	chl IVb
SiO_2	57.63	57.33	55.33	54.15	40.62	52.38	42.02	0.00	54.23	55.41	40.24	0.35	55.93	36.00	29.98
TiO_2	0.13	0.10	0.21	0.29	0.04	0.17	1.31	0.00	0.08	0.23	5.01	0.02	0.19	0.10	0.13
Al_2O_3	0.86	1.20	2.92	3.52	0.00	7.82	16.48	60.80	5.69	3.64	15.50	59.89	2.60	8.48	20.24
Cr_2O_3	0.10	0.17	0.77	0.88	0.00	0.50	1.17	6.43	0.35	0.23	1.00	7.57	0.40	0.22	0.66
Fe_2O_3	n.c.	n.c.	n.c.	n.c.	n.c.	n.c.	0.00	1.22	n.c.	n.c.	0.00	0.00	0.00	n.c.	n.c.
FeO	7.02	7.25	2.84	2.86	9.93	7.75	4.74	11.12	6.83	7.40	4.44	10.94	3.21	8.28	4.32
MnO	0.06	0.27	0.11	0.09	0.19	0.29	0.14	0.08	0.23	0.23	0.07	0.13	0.17	0.21	0.02
NiO	n.a.	n.a.	n.a.	n.a.	0.40	n.a.	n.a.	n.a.	n.a.	n.a.	n.a.	n.a.	n.a.	n.a.	n.a.
MgO	34.53	34.51	18.61	18.11	49.49	30.79	16.68	19.73	32.62	33.09	16.29	19.72	22.55	32.72	31.15
CaO	0.53	0.50	19.54	20.02	0.01	0.75	11.52	0.01	0.59	0.29	11.37	0.07	12.96	0.19	0.05
Na_2O	0.02	0.03	1.36	1.29	0.01	0.08	3.87	0.00	0.03	0.01	3.29	0.00	0.83	0.00	0.00
K_2O	0.00	0.00	0.00	0.01	0.00	0.01	0.06	0.01	0.00	0.00	0.42	0.00	0.02	0.01	0.02
H_2O	–	–	–	–	–	–	2.11	–	–	–	2.09	–	2.19	12.29	12.58
Total	100.88	101.36	101.69	101.22	100.69	100.54	100.10	99.40	100.65	100.53	99.72	98.69	101.05	98.50	99.15
Si	1.975	1.961	1.958	1.932	0.991	1.817	5.981	0.000	1.867	1.912	5.774	0.009	7.641	3.512	2.858
Ti	0.003	0.003	0.005	0.008	0.001	0.004	0.140	0.000	0.002	0.006	0.540	0.000	0.020	0.007	0.010
Al	0.035	0.049	0.122	0.149	0.000	0.320	2.764	1.846	0.231	0.148	2.621	1.830	0.419	0.975	2.274
Cr	0.003	0.005	0.022	0.025	0.000	0.014	0.131	0.131	0.009	0.006	0.113	0.155	0.043	0.017	0.049
Fe^{3+}	n.c.	n.c.	n.c.	n.c.	n.c.	n.c.	0.000	0.024	n.c.	n.c.	0.000	0.000	0.000	n.c.	n.c.
Fe^{2+}	0.201	0.207	0.084	0.085	0.203	0.225	0.565	0.240	0.197	0.214	0.532	0.237	0.367	0.676	0.345
Mn	0.002	0.008	0.003	0.003	0.004	0.009	0.017	0.002	0.007	0.007	0.008	0.003	0.019	0.018	0.001
Ni	n.a.	n.a.	n.a.	n.a.	0.008	n.a.	n.a.	n.a.	n.a.	n.a.	n.a.	n.a.	n.a.	n.a.	n.a.
Mg	1.764	1.760	0.982	0.963	1.801	1.592	3.539	0.758	1.675	1.702	3.485	0.762	4.592	4.759	4.427
Ca	0.020	0.018	0.741	0.765	0.000	0.028	1.756	0.000	0.022	0.011	1.748	0.002	1.897	0.020	0.005
Na	0.001	0.002	0.094	0.090	0.000	0.005	1.067	0.000	0.002	0.001	0.915	0.000	0.220	0.000	0.001
K	0.000	0.000	0.000	0.000	0.000	0.000	0.011	0.000	0.000	0.000	0.077	0.000	0.004	0.001	0.003
Total	4.004	4.013	4.011	4.019	3.008	4.014	15.971	3.001	4.012	4.007	15.831	2.998	15.222	9.985	9.973
XMg	0.898	0.895	0.921	0.919	0.899	0.876	0.862	0.760	0.895	0.888	0.868	0.763	0.926	0.876	0.928

Formula calculations on the basis of 6 oxygens for cpx and opx, 4 oxygens for ol, 12 oxygens for grt, 4 oxygens and 3 cations for spl, and 15 cations without Na + K for am. X_{Mg} for grt, ol, opx, and cpx calculated on the assumption that all Fe is divalent; X_{Mg} for spl and am is calculated using $Fe^{2+}/(Fe^{2+} + Fe^{3+})$ ratio as given by formula calculation. H_2O for am and chl was calculated assuming 2 OH and 8 OH per formula unit, respectively. For mineral abbreviations see section on textures and mineral compositions; c = core, r = rim, n.a. = not analyzed, n.c. = not calculated.

tents and uniform X_{Mg} (Tables 1, 3–7). The rims of larger porphyroclasts have similar X_{Mg} and Cr_2O_3 contents, but may show higher Al_2O_3 contents than the cores (Table 1). CaO contents tend to be lower than those of the cores. Within each sample, opx IIb grains fringing the pseudomorphs after garnet show highly variable compositions with generally low X_{Mg} and high Al_2O_3 and Cr_2O_3. In most garnet pseudomorphs investigated in more detail, Al_2O_3 and Cr_2O_3 contents were found to decrease moving away from the granoblastic layer IIa towards the matrix. Opx IIa grains show significant compositional heterogeneity (Table 1) with no systematic variations, neither between different grains of one pseudomorph nor within individual grains.

Larger cpx I grains have homogeneous cores (Tables 1, 3–7). Rims of larger porphyroclasts and smaller grains show increasing contents of Al_2O_3 and CaO and decreasing Na_2O contents. Clinopyroxenes IIa (only present in peridotites LC and RB) and IIb (only found in peridotite FL) have variable compositions (Table 1).

Relict ol I grains are generally small and have variable X_{Mg} both within and among samples (Ta-

Table 5
Representative electron microprobe analyses of minerals from garnet peridotite FL

	opx Ic	opx Ir	cpx Ic	cpx Ir	ol I	opx IIa	opx IIa	am IIa	spl IIa	opx IIb	opx IIb	chl IVb
SiO_2	57.34	56.77	54.43	53.29	40.72	51.85	55.89	41.79	0.00	53.44	54.75	33.12
TiO_2	0.06	0.14	0.27	0.28	0.03	0.27	0.15	4.20	0.13	0.11	0.13	0.01
Al_2O_3	0.82	1.22	2.80	3.21	0.00	8.05	2.50	13.85	58.56	5.85	3.90	14.28
Cr_2O_3	0.08	0.28	1.01	0.92	0.03	0.42	0.27	0.62	7.06	0.48	0.28	0.31
Fe_2O_3	n.c.	n.c.	n.c.	n.c.	n.c.	n.c.	n.c.	0.00	2.58	n.c.	n.c.	n.c.
FeO	6.62	6.95	3.21	2.73	10.06	8.53	8.45	5.04	12.16	8.02	7.42	11.18
MnO	0.19	0.21	0.08	0.07	0.13	0.29	0.33	0.13	0.25	0.29	0.27	0.46
NiO	n.a.	n.a.	n.a.	n.a.	0.41	n.a.	n.a.	n.a.	n.a.	n.a.	n.a.	n.a.
MgO	33.89	34.27	17.40	16.90	49.03	29.70	32.26	16.59	18.83	30.89	32.13	28.40
CaO	0.61	0.59	18.82	20.85	0.00	0.65	0.31	11.95	0.00	0.73	0.83	0.02
Na_2O	0.03	0.02	1.64	1.05	0.00	0.03	0.03	3.36	0.00	0.00	0.03	0.04
K_2O	0.00	0.00	0.02	0.00	0.00	0.00	0.00	0.21	0.00	0.00	0.00	0.04
H_2O	–	–	–	–	–	–	–	2.09	–	–	–	12.20
Total	99.64	100.45	99.68	99.30	100.41	99.79	100.19	99.83	99.57	99.81	99.74	100.06
Si	1.986	1.958	1.969	1.942	0.996	1.817	1.943	5.994	0.000	1.867	1.908	3.220
Ti	0.002	0.004	0.007	0.008	0.000	0.007	0.004	0.453	0.003	0.003	0.003	0.001
Al	0.033	0.049	0.119	0.138	0.000	0.333	0.103	2.341	1.799	0.241	0.160	1.636
Cr	0.002	0.008	0.029	0.027	0.001	0.011	0.008	0.070	0.145	0.013	0.008	0.024
Fe^{3+}	n.c.	n.c.	n.c.	n.c.	n.c.	n.c.	n.c.	0.000	0.051	n.c.	n.c.	n.c.
Fe^{2+}	0.192	0.200	0.097	0.083	0.206	0.250	0.246	0.604	0.265	0.234	0.216	0.909
Mn	0.005	0.006	0.002	0.002	0.003	0.009	0.010	0.016	0.006	0.009	0.008	0.037
Ni	n.a.	n.a.	n.a.	n.a.	0.008	n.a.	n.a.	n.a.	n.a.	n.a.	n.a.	n.a.
Mg	1.750	1.762	0.938	0.918	1.789	1.552	1.672	3.547	0.732	1.609	1.669	4.116
Ca	0.023	0.022	0.729	0.814	0.000	0.024	0.012	1.836	0.000	0.027	0.031	0.002
Na	0.002	0.001	0.115	0.074	0.000	0.002	0.002	0.934	0.000	0.000	0.002	0.008
K	0.000	0.000	0.001	0.000	0.000	0.000	0.000	0.039	0.000	0.000	0.000	0.005
Total	3.995	4.010	4.006	4.006	3.003	4.005	4.000	15.834	3.001	4.003	4.005	9.958
XMg	0.901	0.898	0.906	0.917	0.897	0.861	0.872	0.854	0.734	0.873	0.885	0.819

Formula calculations on the basis of 6 oxygens for cpx and opx, 4 oxygens for ol, 12 oxygens for grt, 4 oxygens and 3 cations for spl, and 15 cations without Na + K for am. X_{Mg} for grt, ol, opx, and cpx calculated on the assumption that all Fe is divalent; X_{Mg} for spl and am is calculated using $Fe^{2+}/(Fe^{2+} + Fe^{3+})$ ratio as given by formula calculation. H_2O was calculated assuming 2 OH per formula unit for am and 8 OH per formula unit for chl. For mineral abbreviations see section on textures and mineral compositions; c = core, r = rim, n.a. = not analyzed, n.c. = not calculated.

Table 6
Representative electron microprobe analyses of minerals from garnet peridotite LC

	opx Ic	opx Ir	cpx Ic	cpx Ir	ol I	kel	cpx IIa	am IIa	spl IIa	opx IIa	opx IIa	opx IIb	opx III
SiO_2	56.85	56.04	54.54	53.87	40.43	41.05	52.67	41.38	0.00	51.96	54.90	55.02	54.75
TiO_2	0.12	0.15	0.32	0.28	0.02	0.40	0.27	4.77	0.06	0.23	0.12	0.17	0.19
Al_2O_3	0.68	1.38	2.76	2.78	0.01	21.87	3.47	13.75	60.40	7.62	3.18	3.40	2.33
Cr_2O_3	0.15	0.15	0.85	0.93	0.03	1.65	0.95	0.64	7.10	0.40	0.34	0.21	0.11
Fe_2O_3	n.c.	n.c.	n.c.	n.c.	n.c.	n.c.	n.c.	0.00	0.84	n.c.	n.c.	n.c.	n.c.
FeO	6.56	7.09	3.32	2.40	9.92	6.77	3.17	4.58	11.28	8.21	7.15	7.53	7.76
MnO	0.08	0.27	0.04	0.16	0.09	0.21	0.13	0.16	0.09	0.23	0.28	0.23	0.24
NiO	n.a.	n.a.	n.a.	n.a.	0.47	n.a.	n.a.	n.a.	n.a.	n.a.	n.a.	n.a.	n.a.
MgO	34.44	33.40	17.02	16.41	48.95	21.94	18.31	16.15	19.64	30.54	32.33	32.46	32.73
CaO	0.69	0.44	18.75	21.10	0.00	3.93	19.97	11.84	0.03	0.43	0.34	0.55	0.23
Na_2O	0.03	0.00	2.04	1.39	0.01	1.12	0.62	2.92	0.00	0.01	0.00	0.02	0.01
K_2O	0.00	0.00	0.03	0.01	0.01	0.05	0.00	0.48	0.00	0.01	0.00	0.00	0.00
H_2O	–	–	–	–	–	–	–	2.07	–	–	–	–	–
Total	99.60	98.93	99.67	99.33	99.94	98.99	99.56	98.74	99.44	99.64	98.64	99.59	98.35
Si	1.973	1.963	1.975	1.962	0.994	2.946	1.914	5.991	0.000	1.820	1.929	1.919	1.935
Ti	0.003	0.004	0.009	0.008	0.000	0.021	0.007	0.519	0.001	0.006	0.003	0.005	0.005
Al	0.028	0.057	0.118	0.119	0.000	1.851	0.149	2.346	1.836	0.315	0.132	0.140	0.097
Cr	0.004	0.004	0.024	0.027	0.001	0.094	0.027	0.074	0.145	0.011	0.009	0.006	0.003
Fe^{3+}	n.c.	n.c.	n.c.	n.c.	n.c.	n.c.	n.c.	0.000	0.020	n.c.	n.c.	n.c.	n.c.
Fe^{2+}	0.190	0.208	0.101	0.073	0.204	0.406	0.096	0.555	0.243	0.240	0.210	0.220	0.229
Mn	0.002	0.008	0.001	0.005	0.002	0.012	0.004	0.019	0.002	0.007	0.008	0.007	0.007
Ni	n.a.	n.a.	n.a.	n.a.	0.009	n.a.	n.a.	n.a.	n.a.	n.a.	n.a.	n.a.	n.a.
Mg	1.782	1.744	0.919	0.891	1.794	2.346	0.992	3.485	0.755	1.595	1.693	1.688	1.724
Ca	0.026	0.016	0.727	0.823	0.000	0.303	0.778	1.837	0.001	0.016	0.013	0.020	0.009
Na	0.002	0.000	0.143	0.098	0.001	0.157	0.044	0.821	0.000	0.000	0.000	0.001	0.001
K	0.000	0.000	0.001	0.001	0.000	0.005	0.000	0.089	0.000	0.000	0.000	0.000	0.000
Total	4.010	4.004	4.018	4.007	3.005	8.141	4.011	15.736	2.999	4.010	3.997	4.006	4.010
XMg	0.904	0.893	0.901	0.924	0.898	0.852	0.912	0.863	0.757	0.869	0.890	0.885	0.883

Formula calculations on the basis of 6 oxygens for cpx and opx, 4 oxygens for ol, 12 oxygens for grt, 4 oxygens and 3 cations for spl, and 15 cations without Na + K for am. X_{Mg} for grt, ol, opx, and cpx calculated on the assumption that all Fe is divalent; X_{Mg} for spl and am is calculated using $Fe^{2+}/(Fe^{2+} + Fe^{3+})$ ratio as given by formula calculation. H_2O for am was calculated assuming 2 OH per formula unit. For mineral abbreviations see section on textures and mineral compositions; c = core, r = rim, n.a. = not analyzed, n.c. = not calculated.

bles 1, 3–7). Spinel IIa grains are poor in Cr. Plagioclase IIa grains display variable anorthite contents. Amphibole IIa is a K-poor pargasite with variable TiO_2 contents.

Bulk compositions of kelyphites approximate a garnet composition (Tables 3 and 6). As a consequence, the kelyphitization of garnet may be considered as approximately isochemical, with only a minimum of chemical exchange with the surrounding minerals, i.e. small additions of water, Si and Na, and some loss of Fe. Due to the very fine-grained nature of the kelyphites, individual minerals could not always be analyzed. Spinel III is poor in Cr, plg III has variable anorthite contents, and am III is Ti-rich pargasite to kaersutite. Late-stage am IV is tremolitic hornblende (Tables 1, 4, and 7). Chlorite IVa replacing opx IIa or III has lower Al_2O_3 contents and lower X_{Mg} than late-stage chl IVb.

5. Metamorphic evolution and thermobarometry

5.1. Selection of thermometers and barometers

Temperatures were estimated using thermometer formulations based on (1) the enstatite-diopside

solvus (Brey and Köhler, 1990; Bertrand and Mercier, 1985, in a modified form as suggested by Brey and Köhler, 1990) and (2) the amount of Ca in orthopyroxene coexisting with clinopyroxene (Brey and Köhler, 1990). Thermometers based on the Fe–Mg exchange between garnet and pyroxenes or garnet and olivine (e.g., O'Neill and Wood, 1979, 1980; Krogh, 1988; Brey and Köhler, 1990) cannot be used as they are very sensitive to Fe/Mg ratios in garnet and as the exact compositions of the former garnets are not known. As relict garnet grains in peridotite BV are rather small (≤ 300 μm) and in most cases mantled by kelyphite, their Fe/Mg ratios are likely to have been modified. Furthermore, the higher diffusion coefficients for Fe and Mg in most peridotite minerals when compared to Ca and Al (Chakraborty and Ganguly, 1991; Morioka and Nagasawa, 1991; Ganguly and Tazzoli, 1994) imply Fe–Mg exchange down to lower temperatures.

Pressure estimates for garnet-bearing peridotites were obtained with the barometer of Brey and Köhler (1990) which is based on the amount of Tschermak's component in orthopyroxene coexisting with garnet. As no relict garnet was found in peridotites CL, CP,

Table 7
Representative electron microprobe analyses of minerals from garnet peridotite RB

	opx Ic	opx Ir	cpx Ic	cpx Ir	ol I	opx IIa	cpx IIa	am IIa	spl IIa	opx IIb	am IV	phl IV	chl IVb
SiO_2	56.76	57.25	54.52	54.12	40.57	51.65	48.68	43.59	0.02	56.25	55.43	40.08	30.58
TiO_2	0.09	0.09	0.26	0.39	0.01	0.23	1.08	1.31	0.02	0.15	0.26	0.95	0.14
Al_2O_3	1.04	1.51	2.80	3.39	0.01	8.90	10.49	15.66	60.45	2.52	2.41	14.33	18.96
Cr_2O_3	0.25	0.29	0.88	0.52	0.00	0.63	0.84	0.69	6.74	0.10	0.80	0.74	0.62
Fe_2O_3	n.c.	n.c.	n.c.	n.c.	n.c.	n.c.	n.c.	0.56	0.00	n.c.	0.40	n.c.	n.c.
FeO	6.57	6.71	3.72	2.39	10.28	8.42	2.22	2.68	14.31	6.82	1.45	4.30	3.94
MnO	0.11	0.14	0.07	0.12	0.12	0.28	0.05	0.06	0.09	0.16	0.07	0.03	0.06
NiO	n.a.	n.a.	n.a.	n.a.	0.34	n.a.	n.a.	n.a.	n.a.	n.a.	n.a.	n.a.	n.a.
MgO	34.47	34.52	17.84	17.89	49.48	29.90	13.52	18.09	17.37	34.19	22.80	24.69	31.67
CaO	0.74	0.49	18.36	20.74	0.02	0.41	20.94	12.06	0.01	0.57	13.04	0.00	0.02
Na_2O	0.04	0.02	1.60	1.10	0.02	0.03	1.42	2.38	0.04	0.04	0.43	0.00	0.00
K_2O	0.00	0.00	0.04	0.01	0.00	0.01	0.04	0.05	0.00	0.01	0.01	9.26	0.07
H_2O	–	–	–	–	–	–	–	2.12	–	–	2.17	4.24	12.53
Total	100.07	101.02	100.09	100.67	100.85	100.46	99.28	99.25	99.05	100.81	99.27	98.62	98.59
Si	1.962	1.959	1.965	1.939	0.990	1.797	1.777	6.158	0.001	1.931	7.653	2.860	2.928
Ti	0.002	0.002	0.007	0.011	0.000	0.006	0.030	0.139	0.000	0.004	0.027	0.051	0.010
Al	0.042	0.061	0.119	0.143	0.000	0.365	0.451	2.608	1.864	0.102	0.392	1.205	2.139
Cr	0.007	0.008	0.025	0.015	0.000	0.017	0.024	0.077	0.139	0.003	0.087	0.042	0.047
Fe^{3+}	n.c.	n.c.	n.c.	n.c.	n.c.	n.c.	n.c.	0.059	0.000	n.c.	0.041	n.c.	n.c.
Fe^{2+}	0.190	0.192	0.112	0.072	0.210	0.245	0.068	0.317	0.313	0.196	0.167	0.257	0.315
Mn	0.003	0.004	0.002	0.004	0.002	0.008	0.002	0.007	0.002	0.005	0.008	0.002	0.005
Ni	n.a.	n.a.	n.a.	n.a.	0.007	n.a.	n.a.	n.a.	n.a.	n.a.	n.a.	n.a.	n.a.
Mg	1.776	1.760	0.959	0.955	1.800	1.551	0.736	3.809	0.677	1.750	4.694	2.626	4.520
Ca	0.027	0.018	0.709	0.796	0.000	0.015	0.819	1.825	0.000	0.021	1.929	0.000	0.002
Na	0.002	0.001	0.112	0.076	0.001	0.002	0.100	0.652	0.002	0.002	0.116	0.000	0.000
K	0.000	0.000	0.002	0.000	0.000	0.001	0.002	0.009	0.000	0.000	0.002	0.843	0.009
Total	4.011	4.005	4.012	4.011	3.010	4.007	4.009	15.660	2.998	4.014	15.116	7.886	9.975
XMg	0.903	0.902	0.895	0.930	0.896	0.864	0.915	0.923	0.684	0.899	0.966	0.911	0.935

Formula calculations on the basis of 6 oxygens for cpx and opx, 4 oxygens for ol, 12 oxygens for grt, 4 oxygens and 3 cations for spl, and 15 cations without Na + K for am. X_{Mg} for grt, ol, opx, and cpx calculated on the assumption that all Fe is divalent; X_{Mg} for spl and am is calculated using $Fe^{2+}/(Fe^{2+} + Fe^{3+})$ ratio as given by formula calculation. H_2O was calculated assuming 2 OH per formula unit for am and phl and 8 OH per formula unit for chl. For mineral abbreviations see section on textures and mineral compositions; c = core, r = rim, n.a. = not analyzed, n.c. = not calculated.

FL, LC, and RB, a model garnet composition was used for pressure calculations (grt mc in Table 3). This composition was estimated from the near-garnet compositions of kelyphites and from the compositions of relict garnets in garnet peridotite BV. As the Al-in-opx barometer of Brey and Köhler (1990) is not very sensitive to garnet composition and as variations in garnet compositions within the peridotite system are rather limited, this procedure seems justified. For example, pressures calculated at 1100°C for the opx Ic composition of peridotite BV (Table 2) using three different garnet model compositions are very similar: 7.60 GPa with grt I of peridotite BV (Table 2), 8.13 GPa with the grt mc (Table 3), and 7.65 GPa with a garnet composition (grt Z; Table 3) from an ultrahigh-pressure peridotite from eastern China (table 4 in Zhang et al., 1994).

5.2. *Metamorphic stages*

In all six peridotites, stage I is represented by the stable assemblage ol I + opx I + cpx I + grt I. Although pyroxene I compositions show significant intra- and inter-grain heterogeneity, the cores of larger pyroxene porphyroclasts are fairly homogeneous (Fig. 3), indicating that the rocks were once equilibrated within the garnet peridotite stability field. Chemical zoning observed in pyroxene I grains suggests continued growth or partial reequilibration during decompression at slightly increasing or decreasing temperatures.

As the boundaries between inner kelyphites and surrounding coronas are always sharp and as in some peridotites coronas and kelyphites have different assemblages ($\pm$plagioclase, $\pm$clinopyroxene; see Table 1), it is concluded that garnet breakdown occurred in two stages (II and III). First, grt I reacted with ol I, resulting in two-layer coronas around relict garnet: an internal layer with the assemblage opx IIa + am IIa $\pm$ cpx IIa + spl IIa $\pm$ plg IIa adjacent to garnet and an external layer consisting of opx IIb, rarely accompanied by cpx IIb, facing olivine. Stage III corresponds to the near-isochemical breakdown of garnet to fine-grained kelyphites consisting of the assemblages opx III + spl III + am III $\pm$ cpx III (BV) or opx III + spl III + am III + plg III (CL, CP, FL, LC, RB). Stages II and III require the infiltration of H_2O-rich fluids.

Subsequently, continued infiltration of H_2O and minor amounts of CO_2 caused the partial replacement of opx IIa and III by chl IVa and, in peridotites RB and CP, the partial or complete transformation of pseudomorphs after garnet (kelyphites + coronas) to aggregates of chl IVb + am IV $\pm$ calcite $\pm$ graphite. Still later, the rocks were partially serpentinized.

5.3. *P–T conditions*

In the peridotite from *Belle Vue* (*BV*), larger pyroxene I grains show consistent zoning patterns. In opx I, Al and Ca increase from core to rim, whereas in cpx I, Al increases and both Ca and Na decrease from core to rim (Fig. 3). These zoning patterns suggest a decompression that was accompanied by a slight temperature increase. Using the BV grt I composition (Table 2) and combining the 2-px thermometer of Brey and Köhler (1990) with their Al-in-opx barometer (graphically derived best fit) yields temperatures of 960 ± 82°C and pressures of 6.1 ± 0.5 GPa (1σ) for the pyroxene I cores and 1052 ± 80°C/5.1 ± 0.8 GPa for the rims (Table 8). These *P–T* conditions are within the diamond stability field or near to the diamond-graphite phase boundary (Fig. 4). Applying the Ca-in-opx thermometer of Brey and Köhler (1990), instead of the 2-px thermometer, results in 1032 ± 32°C/6.7 ± 0.6 GPa for the cores and 1005 ± 45°C/4.6 ± 0.8 GPa for the rims. Temperatures estimated with the modified version of the 2-px thermometer of Bertrand and Mercier (1985) are significantly lower for both core and rim compositions (Table 8).

The compositional zoning patterns of pyroxene I grains together with the *P–T* data deduced from pyroxene I (and grt I) compositions suggest that after peak pressures had been reached, peridotite BV suffered decompression accompanied by heating. However, some caution is appropriate as a slight hypothetical increase in the Al_2O_3 content of opx I cores would significantly reduce calculated pressures. Furthermore, an isothermal decompression path instead of a decompression accompanied by heating is indicated, if only Ca-in-opx temperatures are considered (Fig. 4 and Table 8).

Small relict opx I and cpx I grains rarely coexisting with relict grt I were also used for *P–T* calculation. For one domain, opx, cpx, and grt yielded

975°C/4.5 GPa (2-px with Al-in-opx; Brey and Köhler, 1990) and 925°C/4.2 GPa (Ca-in-opx and Al-in-opx; Brey and Köhler, 1990). In a second domain, opx and garnet compositions (no cpx present) correspond to 902°C/2.7 GPa (Ca-in-opx with Al-in-opx; Brey and Köhler, 1990). These values indicate grain-size-dependent partial reequilibration during decompression and cooling.

After continued decompression, the assemblage grt I + ol I became unstable and reaction between these phases resulted in the formation of bipartite coronas with seams of opx IIb ± cpx IIb facing

Table 8
Pressure (GPa) and temperature (°C) estimates for garnet peridotites from the Central Vosges Mountains

Assemblage	*T* (2-px BK90)	*P* (Al-opx BK90)	*T* (Ca-opx BK90)	*P* (Al-opx BK90)	*T* (2-px BM85)	*P* (Al-opx BK90)
Belle Vue (BV):						
Ic	960 ± 82	6.1 ± 0.5	1032 ± 32	6.7 ± 0.5	858 ± 56	5.3 ± 0.5
Ir	1052 ± 80	5.1 ± 0.8	1005 ± 45	4.6 ± 0.8	965 ± 65	4.3 ± 0.8
IIa	–	–	816	1.0	–	–
IIb	862–733	1.0	818–773	1.0	835–799	1.0
III	872–811	1.0	860–755	1.0	844–788	1.0
Champ de Laxet (CL):						
Ic	1124 ± 42	5.2 ± 0.3	1050 ± 15	4.6 ± 0.3	1023 ± 51	4.3 ± 0.3
IIa	–	–	816–731	1.0	–	–
IIb	–	–	946–739	1.0	–	–
Col de Perthuis (CP):						
Ic	1103 ± 78	5.0 ± 0.2	1036 ± 17	4.5 ± 0.2	1040 ± 92	4.5 ± 0.2
IIa	–	–	942–720	1.0	–	–
IIb	–	–	866–733	1.0	–	–
III	–	–	776–751	1.0	–	–
Flaconnières (FL):						
Ic	1228 ± 29	5.9 ± 0.1	1106 ± 29	5.0 ± 0.1	1156 ± 45	5.4 ± 0.1
IIa	–	–	1007–766	1.0	–	–
IIb	811–701	1.0	985–898	1.0	780–718	1.0
La Charme (LC):						
Ic	1121 ± 49	5.9 ± 0.3	1108 ± 23	5.8 ± 0.3	1019 ± 56	5.2 ± 0.3
IIa	1105–1075	1.0	914–711	1.0	1099–1057	1.0
IIb	–	–	899–832	1.0	–	–
III	–	–	809–740	1.0	–	–
Roche des Bruyères (RB):						
Ic	1172 ± 48	4.9 ± 0.2	1068 ± 26	4.2 ± 0.2	1090 ± 56	4.4 ± 0.2
IIa	892–869	1.0	914–795	1.0	873–861	1.0
IIb	–	–	940–845	1.0	–	–

Temperatures and pressures for assemblage I are graphically derived best fits that were obtained by combining various thermometers (2-px and Ca-in-opx thermometers of Brey and Köhler, 1990; 2-px thermometer of Bertrand and Mercier, 1985, in a modified version as suggested by Brey and Köhler, 1990) with the Al-in-opx barometer of Brey and Köhler (1990). Errors correspond to 1 σ. For assemblages II and III, temperatures were calculated assuming a pressure of 1.0 GPa. Since the compositions of pyroxenes II and III display significant intra-pseudomorph heterogeneity, temperature ranges instead of averages are given for these assemblages.

olivine and thin layers of opx IIa + cpx IIa ± am IIa + spl IIa facing garnet (stage II). 2-px temperatures and Ca-in-opx temperatures obtained on pyroxenes produced during this stage are between 862 and 773°C at an assumed pressure of 1.0 GPa (Table 8). Al-in-opx pressures calculated with the garnet model composition grt mc (Table 3) are between 1 and 2 GPa, but should be treated with caution as opx IIb

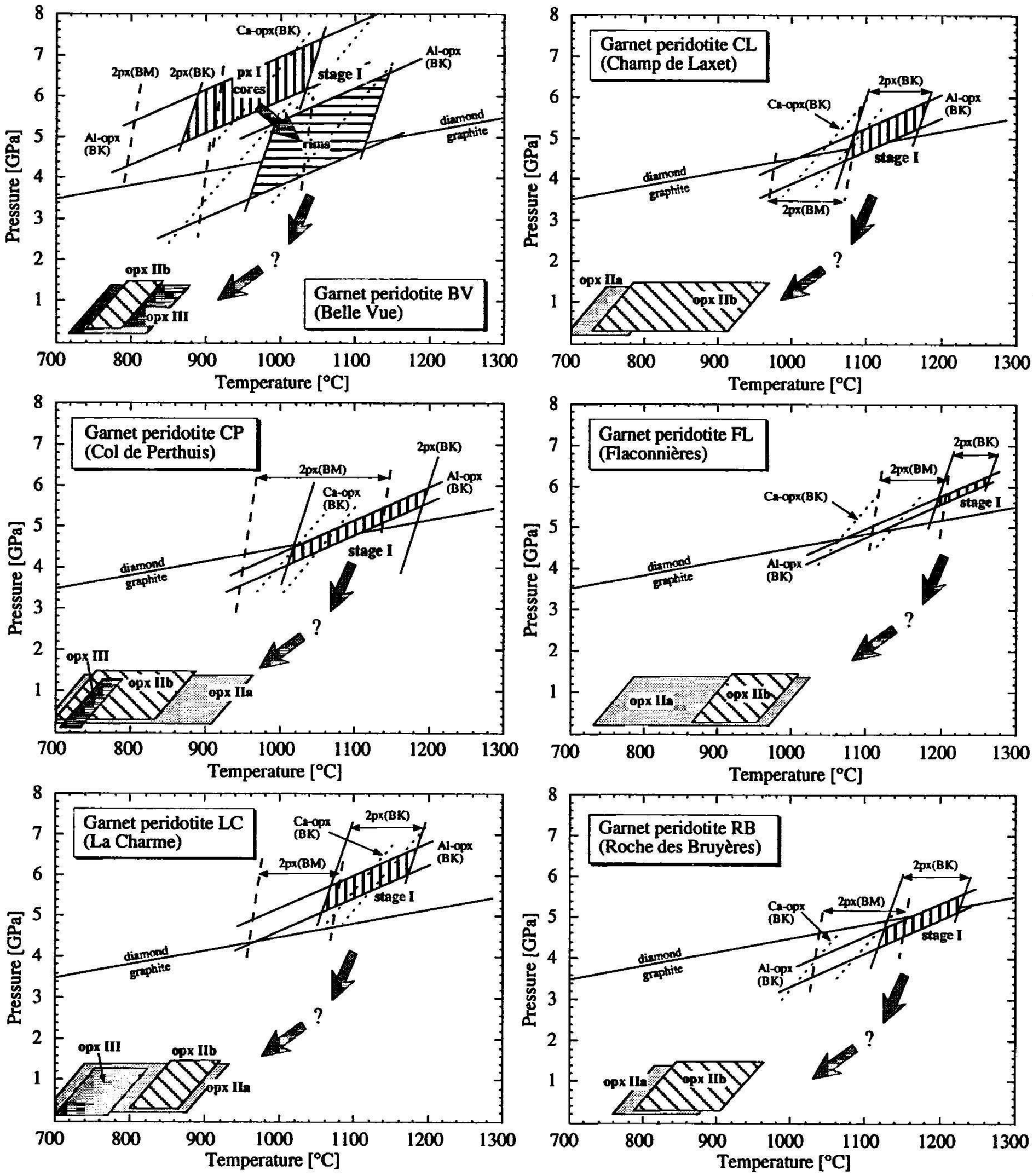

grains were probably not in equilibrium with garnet. Two-pyroxene and Ca-in-opx temperatures obtained for the kelyphite assemblage (am III ± cpx III + opx III + spl III) range from 872 to 755°C (at 1.0 GPa).

In the peridotites from *Champ de Laxet* (*CL*), *Col de Perthuis* (*CP*), *Flaconnières* (*FL*), *La Charme* (*LC*), and *Roche des Bruyères* (*RB*), pyroxene I porphyroclasts show significant compositional heterogeneities (Table 1–7). Core compositions of larger (> 300 μm) porphyroclasts, however, are fairly homogeneous and hence assumed to approximate the original equilibration conditions of the garnet peridotites. Combining the 2-px thermometer (Brey and Köhler, 1990) with the Al-in-opx barometer (Brey and Köhler, 1990) yields temperatures between about 1100 and 1230°C and pressures between 4.9 and 5.9 GPa (Table 8; Fig. 4). Temperatures deduced with the Ca-in-opx thermometer (Brey and Köhler, 1990) and the modified 2-px thermometer of Bertrand and Mercier (1985) are lower and would thus result in lower graphically derived pressures as well (Fig. 4). In any case, also these peridotites were equilibrated either within or near to the diamond stability field.

Core to rim zoning patterns of larger pyroxene porphyroclasts (i.e. Al increasing in both pyroxenes, Ca being nearly constant in opx, but increasing in cpx, Na decreasing in cpx) suggest partial reequilibration during near-isothermal decompression. Partial reequilibration of pyroxene I grains either preceded penetrative deformation or went along with it, as indicated by the fact that larger pyroxene porphyroclasts are strained. As the pseudomorphs after garnet are undeformed in all cases, garnet must have started to break down only after penetrative deformation of the rocks. Reaction of grt I + ol I was accompanied by the infiltration of water and resulted in the formation of reaction coronas consisting of an outer seam of opx IIb ± cpx IIb and an inner zone of opx IIa + am IIa + spl IIa ± cpx IIa ± plg IIa.

Ca-in-opx temperatures and 2-px temperatures obtained for pyroxenes IIa and IIb are variable within each sample and range from 1007 to 701°C at an assumed pressure of 1.0 GPa (Table 8; Fig. 4). Temperatures calculated for pyroxenes of stage III (kelyphites) are in the range of 809–740°C at assumed pressures of 1.0 GPa. High Al contents in opx IIa, IIb and III, and the presence of plagioclase IIa and III (Table 1) suggest low pressures (< 2 GPa) for the beginning of garnet breakdown.

6. Discussion

6.1. Comparison with other Moldanubian garnet peridotite occurrences

Tectonostratigraphic units recognized in the Central Vosges mountains (Latouche et al., 1992) seem to compare well with those from the Bohemian Massif (Medaris et al., 1995a). The same holds true for the high-pressure metamorphic relicts hosted by the different units. In the Bohemian Massif, spinel peridotites are widely distributed in the Monotonous and Varied terranes. In the Vosges, spinel peridotites occur within the comparable Monotonous Group. Within the Bohemian Massif, garnet-bearing peridotites are confined to the granulite-bearing Gföhl terrane (Machart, 1984, 1988; Medaris et al., 1995a; see also Becker, 1996). In the Vosges Mountains, garnet-bearing peridotites are also restricted to a granulite-bearing unit, the Leptynitic granulites. In both massifs, the garnet-bearing peridotites can be split into two groups that are only partly similar. Common to both the 'Leptynitic granulites' of the Vosges Mountains and the Gföhl terrane of the Bohemian Massif are garnet-bearing peridotites with no petrographic indications of pre-existing spinel. Both massifs also contain garnet-spinel peridotites,

Fig. 4. Results of thermobarometric calculations and inferred *P–T* evolutions of garnet peridotites. *P–T* fields for stage I were derived either from core and rim compositions of pyroxene porphyroclasts and relict garnet (BV) or from pyroxene I core compositions and a model garnet composition (CL, CP, FL, LC, RB) using a combination of the 2-px thermometer and the Al-in-opx barometer of Brey and Köhler (1990). *P–T* fields include the $\pm 1\sigma$ range of pressure and temperature values. Temperature ranges obtained with the Ca-in-opx thermometer of Brey and Köhler (1990) and with a modified version of the 2-px thermometer of Bertrand and Mercier (1985) are also depicted. For stages II and III, the ranges of Ca-in-opx temperatures (Brey and Köhler, 1990) are given. The lower and upper pressure limits of these temperature bands are arbitrary. For further explanation and information see section on metamorphic stages and *P–T* conditions in the text and Table 8.

but while those of the Gföhl unit give clear evidence of a former spinel peridotite stage, there is no indication of such a garnet-free stage in the garnet-spinel peridotites of the Vosges Mountains (Altherr and Kalt, in prep.).

Concerning the equilibration conditions of the garnet peridotites, there are differences and similarities between the Leptynitic granulites of the Vosges Mountains and the Gföhl terrane of the Bohemian Massif. Primary equilibration conditions of the Vosgesian garnet peridotites are similar to those obtained for the Nové Dvory garnet peridotite in western Moravia (Medaris et al., 1990) while garnet peridotites from the Gföhl unit of Lower Austria seem to have equilibrated at similar temperatures but somewhat lower pressures (~ 1100°C/3.4 GPa; Carswell, 1991; Becker and Altherr, 1992). The garnet-spinel peridotites of both units show contrasting equilibration conditions. The garnet-bearing rim of the Mohelno spinel peridotite body in the Gföhl unit, for example, shows equilibration at 1070–1265°C and 2.8–2.3 GPa (Medaris et al., 1990). Garnet-spinel peridotites of the Vosges, on the contrary, equilibrated at much lower *P–T* conditions of 700–800°C and 1.6–2.0 GPa (Altherr and Kalt, in prep.).

While there are many similarities in terms of basement lithology and *P–T* conditions between the Central Vosges Mountains and the Bohemian Massif on one side, there are significant differences between the Vosges Mountains and the Schwarzwald, in these respects, on the other. Unfortunately, no subdivision into tectonostratigraphic units has yet been established for the Central Schwarzwald Gneiss Complex (CSGC). This complex contains two types of ultramafic high-pressure rocks displaying contrasting *P–T* evolutions (Kalt et al., 1995; Kalt and Altherr, 1996). Mg–Cr garnet-spinel peridotites equilibrated at 680–770°C/1.4–1.8 GPa compare well to those of the Vosges although they are hosted by a lithologically different unit. Two garnet-websterites with primary equilibration conditions of 740–850°C and 3.2–4.3 GPa, however, have so far no counterparts in the Vosges or elsewhere in the Moldanubian zone. Only one garnet-olivine websterite from the 'Winklarn Series' in the northwestern part of the Bohemian Massif (O'Brien and Schmidt, 1991) may possibly represent an equivalent. Eclogites from the CSGC are of the medium-temperature type (Kalt et al., 1994b) and correspond to those from the Monotonous series of the Bohemian Massif (e.g., O'Brien and Vrána, 1995).

6.2. Origin of Vogesian garnet peridotites and geodynamic consequences

The ultrahigh-pressure garnet peridotites from the Vosges do not provide any evidence for an initial stage at lower pressures. There is no indication of former spinel and all rocks correspond to the Mg–Cr garnet peridotite type as defined by Carswell et al. (1983). These characteristics exclude an origin from former layered basic intrusions as is assumed for some Fe–Ti garnet peridotites from western Norway (Carswell et al., 1983; Jamtveit, 1987a,b). Furthermore, the Vosgesian garnet peridotites do not contain Ti-clinohumite or ilmenite inclusions in olivine thought to indicate former serpentinization and hence derivation from subducted oceanic lithospheric mantle (Evans and Trommsdorff, 1978, 1983). It is therefore possible that the garnet peridotites represent former subcontinental lithospheric mantle that was emplaced into the crust during continental collision.

After equilibration in or near to the diamond stability field, the Vosgesian garnet peridotites followed a *P–T* path characterized by near-isothermal decompression or by an increase in temperature (BV) as pressure decreased. This is indicated by the compositional zoning patterns of pyroxene I grains. The first stage of garnet breakdown (stage II) took place after penetrative deformation of the rocks since the pseudomorphs after garnet are not deformed. Compositions of pyroxenes formed during this stage suggest that temperatures were still high (1000–720°C at an assumed pressure of 1.0 GPa). With the exception of the peridotite BV, garnet breakdown products include plagioclase. All these findings are consistent with the conclusion of these rocks having been transported rapidly from subcontinental upper mantle into the crust with their garnet-bearing assemblage intact.

Rapid exhumation of dense garnet-bearing peridotites can only be achieved by lithospheric extension (e.g. Platt, 1993). Early Carboniferous intracrustal convergence and subsequent initial extension in the Vosges Mountains and the Schwarzwald were accompanied by low-pressure/high-temperature metamorphism (Krohe and Eisbacher, 1988;

Wickert and Eisbacher, 1988; Eisbacher et al., 1989; Wickert et al., 1990; Rey et al., 1991; Echtler and Chauvet, 1992; Echtler and Altherr, 1993; Kalt et al., 1994a). Both the Schwarzwald and the Vosges Mountains are intruded by numerous granitoid plutons dated at 335–310 Ma B.P. (Wendt et al., 1974; Todt, 1976; Hess et al., 1995). Hence, it may be speculated that initial exhumation of the garnet peridotites and their emplacement into the crust were immediately followed or even accompanied by significant heating of the upper mantle and crust.

On a P–T diagram, primary equilibration conditions of the Vosgesian garnet peridotites (Table 8; Fig. 4) plot to the low-temperature side of the adiabatic upwelling curve for normal temperature asthenosphere (potential surface temperature of 1280°C; McKenzie and Bickle, 1989) and suggest that these rocks were once part of a cold high-density lithospheric root. Such roots are convectively unstable and most of their volume is removed into the convecting mantle (e.g., Houseman et al., 1981). Once this has been achieved, surface elevation may increase rapidly. Extension will occur, accompanied by magmatism and evolution towards higher temperature during decompression (e.g., Platt, 1993, and references therein). These features are observed in large parts of the Moldanubian zone. Within such a scenario, the ultrahigh-pressure garnet peridotites of the Vosges may represent those parts of the cold lithospheric root that escaped convective delamination.

7. Conclusions

Three types of Mg–Cr peridotites occur in the Central Vosges Mts.: (1) spinel peridotites, restricted to the lowermost tectonometamorphic unit, the Monotonous Group, (2) garnet-spinel peridotites, and (3) garnet peridotites, the two latter occurring only in the uppermost unit of Leptynitic granulites.

In all Vosgesian garnet peridotites, the oldest discernible stage is documented by partly or completely pseudomorphed garnet and by porphyroclasts of orthopyroxene, clinopyroxene, and olivine. Five out of six investigated peridotite bodies equilibrated at $T \geq 1100$°C$/P \geq 4.9$ GPa within the diamond stability field or near the diamond-graphite phase boundary. Subsequent near-isothermal decompression was accompanied by penetrative deformation resulting in porphyroclastic textures. Continued decompression led to the breakdown of garnet at still elevated temperatures (1000–700°C), accompanied by the infiltration of H_2O.

One garnet peridotite (BV) equilibrated at slightly different P–T conditions (960°C/6.1 GPa) well within the diamond stability field. For this rock, a clockwise P–T path with a slight increase in temperature during the initial stages of decompression is suggested by compositional zoning patterns of pyroxenes. Garnet breakdown also occurred at elevated temperatures but no plagioclase was produced.

From the inferred P–T paths, it is suggested that the garnet peridotites were emplaced into the crust rapidly and with their garnetiferous assemblages intact. Most probably, the exhumed garnet lherzolites are derived from a Variscan lithospheric root.

In a general sense, subdivision of basement units as well as nature and equilibration conditions of garnet peridotites in the Vosges are similar to those of the Bohemian Massif, while they contrast markedly with those of the Schwarzwald.

Acknowledgements

We thank Hans-Peter Meyer for help with the microprobe work and with formula and P–T calculation programs. Technical support was provided by Ilona Salzmann, Udo Geilenkirchen, and Dieter Scholz. Reviews by Patrick J. O'Brien, Gerhard Franz, and Gordon Medaris are much appreciated. This is a contribution to the German National Research Project 'Orogenic Processes with particular reference to the Variscides'.

References

Altherr, R. and Kalt, A., 1995. Metamorphic evolution of Hercynian garnet-bearing peridotites from the Vosges Mts. (France) and the Schwarzwald (Germany). Eur. J. Mineral., 7(1): 5.

Becker, H., 1996. Geochemistry of garnet peridotite massifs from lower Austria and the composition of deep lithosphere beneath a Paleozoic convergent plate margin. In: M.A. Menzies et al. (Editors), Melt Processes and Exhumation of Garnet, Spinel and Plagioclase Facies Mantle. Chem. Geol., 134: 49–65 (this issue).

Becker, H. and Altherr, R., 1992. Evidence from ultra-high-pressure marbles for recycling of sediments into the mantle. Nature (London), 358: 745–748.

Bertrand, P. and Mercier, J-M.M., 1985. The mutual solubility of coexisting ortho- and clinopyroxene: towards an absolute geothermometer for the natural system? Earth Planet. Sci. Lett., 76: 109–122.

Bonhomme, M., 1965. Age, par la méthode au strontium de quelques granites des Vosges moyennes. Sci. Terre, 10: 385–393.

Bonhomme, M., 1967. Ages radiométriques de quelques granites des Vosges moyennes. Bull. Serv. Carte Géol. Alsace Lorraine, 20: 101–106.

Bonhomme, M. and Fluck, P., 1981. Nouvelles données isotopiques Rb–Sr obtenues sur les granulites des Vosges. Age protérozoïques terminal de la série volcanique calcoalcaline et âge acadien du métamorphisme régional. C.R. Acad. Sci., Paris, Sér. II, 293: 771–774.

Brey, G.P. and Köhler, T., 1990. Geothermobarometry in four-phase lherzolites II. New thermobarometers, and practical assessment of existing thermobarometers. J. Petrol., 31: 1353–1378.

Carswell, D.A., 1991. Variscan high $P-T$ metamorphism and uplift history in the Moldanubian Zone of the Bohemian Massif in Lower Austria. Eur. J. Mineral., 3: 323–342.

Carswell, D.A. and Gibb, F.G.F., 1980. The equilibration conditions and petrogenesis of European crustal garnet lherzolites. Lithos, 13: 19–29.

Carswell, D.A., Harvey, M.A. and Al-Samman, A., 1983. The petrogenesis of contrasting Fe–Ti and Mg–Cr garnet peridotite types in the high grade gneiss complex of western Norway. Bull. Minéral., 106: 727–750.

Chakraborty, S. and Ganguly, J., 1991. Compositional zoning and cation diffusion in garnet. In: J. Ganguly (Editor), Diffusion, Atomic Ordering and Mass Transport. Springer, New York, N.Y., pp. 120–175.

Echtler, H.P. and Altherr, R., 1993. Variscan crustal evolution in the Vosges Mountains and in the Schwarzwald: Guide to the excursion of the Swiss Geological Society and the Swiss Society of Mineralogy and Petrology (3–5 October, 1992). Schweiz. Mineral. Petrogr. Mitt., 73: 113–128.

Echtler, H.P. and Chauvet, A., 1992. Carboniferous convergence and subsequent crustal extension in the southern Schwarzwald (SW Germany). Geodin. Acta, 5: 37–49.

Eisbacher, G.H., Lüschen, E. and Wickert, F., 1989. Crustal-scale thrusting and extension in the Hercynian Schwarzwald and Vosges, Central Europe. Tectonics, 8: 1–21.

Ernst, W.G., 1978. Petrochemical study of lherzolitic rocks from the Western Alps. J. Petrol., 19: 341–392.

Evans, B.W. and Trommsdorff, V., 1978. Petrogenesis of garnet lherzolite, Cima di Gagnone, Lepontine Alps. Earth Planet. Sci. Lett., 40: 333–348.

Evans, B.W. and Trommsdorff, V., 1983. Fluorine Hydroxyl Titanian Clinohumite in Alpine recrystallized garnet peridotite: compositional controls and petrologic significance. Am. J. Sci., 283: 355–369.

Fabriès, J. and Latouche, L., 1988. Granulite facies conditions in the Ste-Marie-aux-Mines 'Varied Group' (Central Vosges, France). Terra Cognita, 8(3): 249.

Faul, H. and Jäger, E., 1963. Ages of some granitic rocks in the Vosges, the Schwarzwald and the Massif Central. J. Geophys. Res., 68: 3293–3300.

Fluck, J.P., 1980. Métamorphisme et magmatisme dans les Vosges moyennes d'Alsace. Contributions à l'histoire de la chaîne varisque. Sci. Géol. Strasbourg, Mem. 62.

Ganguly, J. and Tazzoli, V., 1994. Fe^{2+}–Mg interdiffusion in orthopyroxene: retrieval from the data on intercrystalline exchange reaction. Am. Mineral., 79: 930–937.

Hameurt, J., 1967. Les terrains cristallins et cristallophylliens du versant occidental des Vosges moyennes. Mem. Serv. Carte Géol. Alsace Lorraine, 26: 1–402.

Hameurt, J. and Vidal, P., 1973. Contribution de la géochemie isotopique du strontium à la connaissance du socle des Vosges. Bull. Soc. Géol. Fr., Sér. 7, 15: 246–251.

Hess, J.C., Lippolt, H.J. and Kober, B., 1995. The age of the Kagenfels granite (northern Vosges) and its bearing on the intrusion scheme of late Variscan granitoids. Geol. Rundsch., 84: 568–577.

Houseman, G.A., McKenzie, D.P. and Molnar, P., 1981. Convective instability of a thickened boundary layer and its relevance for the thermal evolution of continental convergence belts. J. Geophys. Res., 86: 6115–6132.

Jamtveit, B., 1987a. Metamorphic evolution of the Eiksunddal eclogite complex, western Norway, and some tectonic implications. Contrib. Mineral. Petrol., 95: 82–99.

Jamtveit, B., 1987b. Magmatic and metamorphic controls on chemical variations within the Eiksunddal eclogite complex, Sunnmøre, western Norway. Lithos, 20: 369–389.

Kalt, A. and Altherr, R., 1996. Metamorphic evolution of garnet-spinel peridotites from the Variscan Schwarzwald (F.R.G.). Geol. Rundsch., 85: 211–224 .

Kalt, A., Grauert, B. and Baumann, A., 1994a. Rb–Sr and U–Pb studies on migmatites from the Schwarzwald (F.R.G.): constraints on isotopic resetting during high-temperature metamorphism. J. Metamorph. Geol., 12: 667–680.

Kalt, A., Hanel, M., Schleicher, H. and Kramm, U., 1994b. Petrology and geochronology of eclogites from the Variscan Schwarzwald (F.R.G.). Contrib. Mineral. Petrol., 115: 287–302.

Kalt, A., Altherr, R. and Hanel, M., 1995. Contrasting $P-T$ conditions recorded in ultramafic high-pressure rocks from the Variscan Schwarzwald (F.R.G.). Contrib. Mineral. Petrol., 121: 45–60.

Kossmat, F., 1927. Gliederung des varistischen Gebirgsbaues. Abh. Sächs. Geol. L.-A., 1: 1–39.

Krogh, E.J., 1988. The garnet-clinopyroxene Fe–Mg geothermometer—reinterpretation of existing experimental data. Contrib. Mineral. Petrol., 99: 44–48.

Krohe, A. and Eisbacher, G.H., 1988. Oblique crustal detachment in the Variscan Schwarzwald, southwestern Germany. Geol. Rundsch., 77: 25–43.

Latouche, L., Fabriès, J. and Guiraud, M., 1992. Retrograde evolution in the Central Vosges mountains (northeastern France): implications for the metamorphic history of high-grade

rocks during the Variscan orogeny. Tectonophysics, 205: 387–407.

Machart, J., 1984. Ultramafic rocks in the Bohemian part of the Moldanubicum and central Bohemian islet zone (Bohemian massif). Krystalinikum, 17: 13–32.

Machart, J., 1988. Petrology and position of ultramafic rocks in the Moldanubian region of the Bohemian Massif. In: V. Zoubek, J. Cogné, D. Kozhoukharov and H.G. Kräutner (Editors), Precambrian in Younger Fold Belts. Wiley, New York, N.Y., pp. 233–238.

McKenzie, D. and Bickle, M.J., 1989. The volume and composition of melt generated by extension of the lithosphere. J. Petrol., 29: 625–679.

Medaris, L.G., 1980a. Convergent metamorphism of eclogite and garnet-bearing ultramafic rocks at Lien, west Norway. Nature (London), 283: 470–472.

Medaris, L.G., 1980b. Petrogenesis of the Lien peridotite and associated eclogites, Almklovdalen, western Norway. Lithos, 13: 339–353.

Medaris, L.G. and Carswell, D.A., 1990. Petrogenesis of Mg–Cr garnet peridotites in European metamorphic belts. In: D.A. Carswell (Editor), Eclogite Facies Rocks. Blackie, Glasgow, pp. 260–290.

Medaris, L.G., Jr., Wang, H.F., Mísař, Z. and Jelínek, E., 1990. Thermobarometry, diffusion modelling and cooling rates of crustal garnet peridotites. Two examples from the Moldanubian zone of the Bohemian Massif. Lithos, 25: 189–202.

Medaris, L.G., Beard, B.L., Johnson, C.M., Valley, J.W., Spicuzza, M.J., Jelínek, E. and Mísař, Z., 1995a. Garnet pyroxenite and eclogite in the Bohemian Massif: geochemical evidence for Variscan recycling of subducted lithosphere. Geol. Rundsch., 84: 489–505.

Medaris, Jr., L.G., Jelínek, E. and Mísař, Z., 1995b. Czech eclogites — Terrane settings and implications for Variscan tectonic evolution of the Bohemian Massif. Eur. J. Mineral., 7: 7–28.

Montigny, R. and Thuizat, R., 1989. K–Ar and ^{40}Ar–^{39}Ar ages on crystalline rocks of the Vosges (France). Terra Abstr., 1: 352.

Montigny, R., Schneider, C., Royer, J.Y. and Thuizat, R., 1983. K–Ar dating of some plutonic rocks of the Vosges, France. Terra Cognita, 3: 201.

Morioka, M. and Nagasawa, H., 1991. Ionic diffusion in olivine. In: J. Ganguly (Editor), Diffusion, Atomic Ordering and Mass Transport. Springer, New York, N.Y., pp. 176–197.

O'Brien, P.J. and Carswell, D.A., 1993. Tectonometamorphic evolution of the Bohemian Massif: evidence from high-pressure metamorphic rocks. Geol. Rundsch., 82: 531–555.

O'Brien, P.J. and Schmidt, I., 1991. The multistage metamorphic evolution of a retrograded garnet websterite from the Variscan basement of the Oberpfalz, NE Bavaria, Germany. Terra Abstr., 3: 94.

O'Brien, P.J. and Vrána, S., 1995. Eclogites with a short-lived granulite facies overprint in the Moldanubian Zone, Czech Republic: petrology, geochemistry and diffusion modelling of garnet zoning. Geol. Rundsch., 84: 473–488.

O'Neill, H., StC. and Wood, B.J., 1979. An experimental study of Fe–Mg partitioning between garnet and olivine and its calibration as a geothermometer. Contrib. Mineral. Petrol., 70: 59–70.

O'Neill, H., StC. and Wood, B.J., 1980. An experimental study of Fe–Mg partitioning between garnet and olivine and its calibration as a geothermometer: corrections. Contrib. Mineral. Petrol., 72: 337.

Obata, M., 1980. The Ronda peridotite: garnet-, spinel-, and plagioclase-lherzolite facies and the P–T trajectories of a high-temperature mantle intrusion. J. Petrol., 21: 533–572.

Platt, J.P., 1993. Exhumation of high-pressure rocks: a review of concepts and processes. Terra Nova, 5: 119–133.

Rey, P., Burg, J.-P., Lardeaux, J.-M. and Fluck, P., 1989. Evolutions métamorphiques contrastées dans les Vosges orientales: témoins d'un charriage dans la chaine varisque. C.R. Acad. Sci. Paris, Sér. II, 309: 815–821.

Rey, P., Burg, J.-P. and Caron, J.-M., 1991. Tectonique extensive ductile et plutonisme viséo-namurien dans les Vosges. C.R. Acad. Sci. Paris, Sér. II, 312: 1609–1616.

Todt, W., 1976. Zirkon U/Pb-Alter des Malsburg-Granits vom Südschwarzwald. Neues Jahrb. Mineral. Monatsh., pp. 532–544.

Wang, X., Zhang, R.Y. and Liou, J.G., 1995. Ultrahigh-pressure metamorphic terrane in eastern central China. In: R.G. Coleman and X. Wang (Editors), Ultrahigh-Pressure Metamorphism. Cambridge University Press, Cambridge, pp. 356–390.

Wendt, I., Lenz, H. and Höhndorf, A., 1974. Das Alter des Bärhalde-Granites (Schwarzwald) und der Uranlagerstätte Menzenschwand. Geol. Jahrb., E2: 131–143.

Werling, F. and Altherr, R., 1991. Sapphirine as a breakdown product of garnet in a former garnet peridotite from the Vosges Mountains, France. Terra Abstr., 3: 437–438.

Wickert, F. and Eisbacher, G.H., 1988. Two-sided Variscan thrust tectonics in the Vosges Mountains, northeastern France. Geodin. Acta, 2: 101–120.

Wickert, F., Altherr, R. and Deutsch, M., 1990. Polyphase Variscan tectonics and metamorphism along a segment of the Saxothuringian–Moldanubian boundary: the Baden–Baden Zone, northern Schwarzwald (F.R.G.). Geol. Rundsch., 79: 627–647.

Zhang, R.Y., Liou, J.G. and Cong, B.L., 1994. Petrogenesis of garnet-bearing ultramafic rocks and associated eclogites in the Su-Lu ultrahigh-P metamorphic terrane, eastern China. J. Metamorph. Geol., 12: 169–186.

Zhang, R.Y., Liou, J.G. and Cong, B.L., 1995. Talc-, magnesite- and Ti-clinohumite-bearing ultrahigh-pressure meta-mafic and ultramafic complex in the Dabie Mountains, China. J. Petrol., 36: 1011–1037.